



UPPSALA
UNIVERSITET

*Digital Comprehensive Summaries of Uppsala Dissertations
from the Faculty of Science and Technology 1618*

Measurements of X-Ray Emission from Laboratory Sparks and Upward Initiated Lightning

PASAN HETTIARACHCHI



ACTA
UNIVERSITATIS
UPSALIENSIS
UPPSALA
2018

ISSN 1651-6214
ISBN 978-91-513-0204-1
urn:nbn:se:uu:diva-338158

Dissertation presented at Uppsala University to be publicly examined in 80127, Ångströmlaboratoriet, Lägerhyddsvägen 1, Uppsala, Tuesday, 27 February 2018 at 09:00 for the degree of Doctor of Philosophy. The examination will be conducted in English. Faculty examiner: Professor Marcos Rubinstein (University of Applied Sciences of Western Switzerland, Institute for Information and Communication Technologies).

Abstract

Hettiarachchi, P. 2018. Measurements of X-Ray Emission from Laboratory Sparks and Upward Initiated Lightning. *Digital Comprehensive Summaries of Uppsala Dissertations from the Faculty of Science and Technology* 1618. 58 pp. Uppsala: Acta Universitatis Upsaliensis. ISBN 978-91-513-0204-1.

In 1925 Nobel laureate R. C. Wilson predicted that high electric fields of thunderstorms could accelerate electrons to relativistic energies which are capable of generating high energetic radiation. The first detection of X-rays from lightning was made in 2001 and from long sparks in 2005. Still there are gaps in our knowledge concerning the production of X-rays from lightning and long sparks, and the motivation of this thesis was to rectify this situation by performing new experiments to gather data in this subject.

The first problem that we addressed in this thesis was to understand how the electrode geometry influences the generation of X-rays. The results showed that the electrode geometry affects the X-ray generation and this dependency could be explained using a model developed previously by scientists at Uppsala University. The other missing information was the distribution of energy. Using a series of attenuators, we observed how the X-ray photons were attenuated as a function of barrier thickness and using a simple model we obtained the average and the maximum energy of X-rays.

All the studies conducted previously was based on the lightning impulses, but in switching impulses, the voltage waveform rises very slowly compared to lightning impulses, and according to some scientists the rate of rise is an important parameter in X-ray development. Our study showed that the switching impulses were as efficient as lightning impulses in generating X-rays even though the rate of rise of voltage in switching impulses was hundreds of times slower.

All the observations on X-ray generation from lightning by other scientists were based on either natural downward lightning flashes or triggered lightning in Florida. The first experiments to study the X-ray generation from upward lightning flashes systematically was conducted within this thesis work at Gaisberg Tower in Austria. The results showed that the X-ray emissions from these flashes were much weaker than the ones produced by either natural downward or triggered lightning. An attempt was made to explain this observation by invoking the possible differences in the charge distribution of leaders associated with the triggered lightning flashes in Florida and upward initiated lightning flashes at Gaisberg tower.

Keywords: X-ray, upward lighting, laboratory discharges, energy distribution

Pasan Hettiarachchi, Department of Engineering Sciences, Electricity, Box 534, Uppsala University, SE-75121 Uppsala, Sweden.

© Pasan Hettiarachchi 2018

ISSN 1651-6214

ISBN 978-91-513-0204-1

urn:nbn:se:uu:diva-338158 (<http://urn.kb.se/resolve?urn=urn:nbn:se:uu:diva-338158>)

To Mehasna and Kinuli

List of Papers

This thesis is based on the following papers, which are referred to in the text by their Roman numerals.

- I **Hettiarachchi, P.;** Rahman, M.; Cooray, V.; Dwyer, J. X-rays from negative laboratory sparks in air: Influence of the anode geometry. *J. Atmos. Solar-Terrestrial Phys.* **2017**, *154*, 190–194, doi:10.1016/j.jastp.2016.07.012.

Part of this work was presented at International Conference on Atmospheric Electricity ICAE 2014, Norman, OK, U.S.A.

- II **Hettiarachchi, P.;** Cooray, V.; Rahman, M.; Dwyer, J. Energy Distribution of X-rays Produced by Meter-Long Negative Discharges in Air. *Atmosphere (Basel)*. **2017**, *8*, 244, doi:10.3390/atmos8120244.

- III **Hettiarachchi, P.;** Cooray, V.; Diendorfer, G.; Pichler, H.; Dwyer, J.; Rahman, M. X-ray Observations at Gaisberg Tower. *Atmosphere (Basel)*. **2018**, *9*, 20, doi:10.3390/atmos9010020.

- IV Rahman, M., **Hettiarachchi, P.**, Cooray, V., Dwyer, J., Rassoul, H., & Rakov, V. X-ray observations from laboratory sparks in air at atmospheric pressure under negative switching impulse voltages. *Manuscript*. **2018**

Part of this work was presented at the 33rd International Conference on Lightning Protection, ICLP2016, Estoril, Portugal.

Reprints were made with permission from the respective publishers.

Selected contributions during doctoral studies of the author, which are not included in this thesis are given below.

Book Chapters:

- I Cooray, V.; **Hettiarachchi, P.**; Cooray, G. Basic electromagnetic theory - A summary. In *Lightning Electromagnetics*; IET: Stevenage, UK, **2012**; pp. 1–53 ISBN 9781849192163.

Journal Articles:

- II Johari, D.; Cooray, V.; Rahman, M.; **Hettiarachchi, P.**; Ismail, M. M. Characteristics of leader pulses in positive ground flashes in Sweden. *Electr. Power Syst. Res.* **2017**, *153*, 3–9, doi:10.1016/j.epsr.2016.11.026.
- III Ismail, M. M.; Rahman, M.; Cooray, V.; Fernando, M.; **Hettiarachchi, P.**; Johari, D. On the possible origin of chaotic pulse trains in lightning flashes. *Atmosphere (Basel)*. **2017**, *8*, doi:10.3390/atmos8020029.
- IV Johari, D.; Cooray, V.; Rahman, M.; **Hettiarachchi, P.**; Ismail, M. M. Features of the first and the subsequent return strokes in positive ground flashes based on electric field measurements. *Electr. Power Syst. Res.* **2017**, *150*, doi:10.1016/j.epsr.2017.04.-031.
- V Diaz, O.; **Hettiarachchi, P.**; Rahman, M.; Cooray, V.; Vayanganie, S. P. A. Experimental study of leader tortuosity and velocity in long rod-plane air discharges. *IEEE Trans. Dielectr. Electr. Insul.* **2016**, *23*, doi:10.1109/TDEI.2015.005421.
- VI Vayanganie, S. P. A.; Cooray, V.; Rahman, M.; **Hettiarachchi, P.**; Diaz, O.; Fernando, M. On the occurrence of “bead lightning” phenomena in long laboratory sparks. *Phys. Lett. Sect. A Gen. At. Solid State Phys.* **2016**, *380*, doi:10.1016/j.physleta.2015.12.039.
- VII Johari, D.; Cooray, V.; Rahman, M.; **Hettiarachchi, P.**; Ismail, M. M. Characteristics of preliminary breakdown pulses in positive ground flashes during summer thunderstorms in Sweden. *Atmosphere (Basel)*. **2016**, *7*, doi:10.3390/atmos7030039.
- VIII Baharudin, Z. A.; Cooray, V.; Rahman, M.; **Hettiarachchi, P.**; Ahmad, N. A. On the characteristics of positive lightning ground flashes in Sweden. *J. Atmos. Solar-Terrestrial Phys.* **2016**, *138–139*, doi:10.1016/j.jastp.2015.12.014.
- IX Ahmad, M. R.; Esa, M. R. M.; Cooray, V.; Baharudin, Z. A.; **Hettiarachchi, P.** Latitude dependence of narrow bipolar pulse emissions. *J. Atmos. Solar-Terrestrial Phys.* **2015**, *128*, 40–45, doi:10.1016/j.jastp.2015.03.005.

- X Ismail, M. M.; Rahman, M.; Cooray, V.; Sharma, S.; **Hettiarachchi, P.**; Johari, D. Electric field signatures in wideband, 3 MHz and 30 MHz of negative ground flashes pertinent to Swedish thunderstorms. *Atmosphere (Basel)*. **2015**, 6, doi:10.3390/atmos6121837.

Peer Reviewed Conference Proceedings:

- XI Ismail, M. M., Cooray, V., Rahman, M., **Hettiarachchi, P.**, & Johari, D. (2017). Wavelet transform reveals the origin of chaotic pulse train in lightning flashes. In *4th International Symposium on Winter Lightning (ISWL2017)*, Joetsu, Japan, April 2017.
- XII Johari, D., Cooray, V., Rahman, M., **Hettiarachchi, P.**, & Ismail, M. (2017). Some features of preliminary breakdown pulses in positive ground flashes in Sweden. In *4th International Symposium on Winter Lightning (ISWL2017)*, Joetsu, Japan, April 2017.
- XIII Ismail, M. M., Rahman, M., Cooray, V., **Hettiarachchi, P.**, & Johari, D. (2017). Characteristics of chaotic pulse trains associated with dart and dart-stepped leader in lightning flashes in Sweden. In *4th International Symposium on Winter Lightning (ISWL2017)*, Joetsu, Japan, April 2017.
- XIV Vayanganie, S. P. A.; Gunasekara, L.; Fernando, M.; Sonnadara, U.; Cooray, V.; Rahman, M.; **Hettiarachchi, P.** Fractal Analysis of Long Laboratory Sparks of high Speed Video Recordings. In *33rd International Conference on Lightning Protection, ICLP2016*; 2016.
- XV Rahman, M.; **Hettiarachchi, P.**; Cooray, V.; Dwyer, J. R.; Rasoul, H. K. Production of X-rays in Air Gaps Stressed by Switching Impulse Voltages. In *33rd International Conference on Lightning Protection, ICLP2016*; 2016.
- XVI Saba, M. M. F.; Naccarato, K. P.; Paiva, A. R. De; Schumann, C.; Cooray, V.; **Hettiarachchi, P.**; Diendorfer, G.; Piantini, A.; Claudio, J.; Oliveira, D. The study of lightning strikes to common buildings in Brazil. In *33rd International Conference on Lightning Protection, ICLP2016*; 2016.
- XVII Chandimal, A. P. L.; Nanayakkara, S.; Fernando, M.; **Hettiarachchi, P.**; Cooray, V.; Rahman, M. Special Attention to Impedance of Conductivity Enhancing Backfill Materials. In *33rd International Conference on Lightning Protection, ICLP2016*; 2016.

- XVIII Johari, D., Cooray, V., Rahman, M., **Hettiarachchi, P.**, & Ismail, M. (2016). Some characteristics of subsequent return strokes in positive ground flash in Sweden. In *International Conference on Lightning Protection, ICLP2016, Estoril, Portugal*.
- XIX Ismail, M., Cooray, V., Rahman, M., **Hettiarachchi, P.**, & Johari, D. (2016). On comparison between initial breakdown pulses and narrow bipolar pulses in lightning discharges with special attention to electric field derivative characteristics. In *International Conference on Lightning Protection, ICLP2016, Estoril, Portugal*.
- XX Johari, D., Cooray, V., **Hettiarachchi, P.**, Rahman, M., & Ismail, M. M. (2015). Some characteristics of leader pulses in positive cloud-to-ground flashes. In *2015 International Symposium on Lightning Protection, XIII SIPDA 2015*.
- XXI Ismail, M. M., Cooray, V., **Hettiarachchi, P.**, Rahman, M., Fernando, M., & Johari, D. (2015). On the possible origin of chaotic pulse trains in lightning flashes. In *2015 International Symposium on Lightning Protection, XIII SIPDA 2015*.
- XXII **Hettiarachchi, P.**; Rahman, M.; Cooray, V. X-rays from long laboratory sparks: Influence of the anode geometry. In *International Conference on Atmospheric Electricity ICAE 2014, Norman, OK, U.S.A.; 2014*.
- XXIII Ahmad, M. R., Esa, M. R. M., **Hettiarachchi, P.**, & Cooray, V. (2012). Preliminary observations of lightning signature at 2400 MHz in Sweden thunderstorm. In *2012 IEEE Asia-Pacific Conference on Applied Electromagnetics, APACE 2012 - Proceedings*.

Contents

1.	Introduction	13
1.1.	High energetic radiation with atmospheric origin	13
1.2.	Observations, measurements and possible source mechanisms	13
2.	Background, motivations, and the objectives	15
2.1.	Understanding the effect of electrode geometry.....	15
2.2.	The energy distribution of X-ray photons	16
2.3.	X-rays produced by upward initiated lightning flashes.....	17
2.4.	X-rays produced by switching impulses.....	18
3.	Methodology.....	19
3.1.	A typical scintillation X-ray detection system	19
3.1.1	Principle of operation.....	19
3.1.2	The complete detection system.....	20
3.1.3	Efficiency of a scintillation X-ray detector system.....	21
3.1.4	Rise and decay times of a detector and their implications.....	21
3.1.5	Calibration of X-ray detector system.....	22
3.1.6	The effect of background radiation and statistical probability of false detections.....	24
3.2.	Influence of the anode geometry in X-ray production (Paper I)	25
3.2.1.	Experimental setup	25
3.3.	Energy distribution of X-rays from laboratory discharges (Paper II)	26
3.3.1.	Experimental Setup.....	26
3.3.2.	Numerical model of X-ray attenuation	27
3.4.	X-rays produced by upward initiated lightning (Paper III)	29
3.4.1.	Experimental setup	29
3.5.	X-rays produced by switching impulses (Paper IV).....	30
3.5.1.	Experimental setup	31
4.	Results and Discussions.....	33
4.1.	What is the role of the grounded anode? (Paper I)	33
4.1.1.	Energetic X-rays produced with a smaller anode	34
4.1.2.	Does streamer encounter produce X-rays?	34
4.2.	What are the probable X-ray energy distributions? (Paper II) ...	35
4.2.1.	Average energy vs. attenuator thickness.....	35
4.2.2.	Probable energy distributions	36

4.2.3.	Kramers' law as a distribution	37
4.2.4.	Exponential distribution.....	37
4.2.5.	Comparison of distributions and concluding remarks	40
4.3.	X-rays observation at Gaisberg Tower (Paper III)	41
4.3.1.	Results of the experiment	41
4.3.2.	What are the reasons for the weak X-ray production?.....	43
4.4.	X-rays produced by switching impulses (Paper IV).....	44
4.4.1.	X-rays produced by horizontal sphere-sphere gap.....	44
4.4.2.	X-rays produced by vertical sphere-sphere gap.....	46
4.4.3.	X-rays produced by vertical rod-plane gap.....	46
4.4.4.	The origin of X-rays and comparison to X-ray production from lightning impulses.....	46
5.	Conclusions	48
6.	Future Work.....	50
	Svensk Sammanfattning.....	52
	Acknowledgements.....	54
	References.....	56

Abbreviations and nomenclature

ALDIS	Austrian Lightning Detection and Information System
BATSE	Burst and Transient Source Experiment
EMC	Electromagnetic Compatibility
HV	High Voltage
ICC	Initial Continuing Current
NaI(Tl)	Thallium doped Sodium Iodide
NIST	National Institute of Standards and Technology (USA)
PMT	Photo Multiplier Tube
TGF	Terrestrial Gamma-Ray Flash
fluence	A measurement of radiant exposure (measured by photons/cm ² or MeV/cm ²)
$(\mu/\rho)_m$	Mass attenuation coefficient of any given material 'm' for X-rays; depends on the energy of X-ray photons and the material itself.

1. Introduction

1.1. High energetic radiation with atmospheric origin

Measurements and observations made starting from the last decade of the 20th century have revealed many unknown processes in our atmosphere capable of generating high energetic radiation. These processes are still beyond our current understanding. They emit radiation in different time scales and intensities such as X-ray bursts in sub-microsecond duration, gamma-ray flashes called Terrestrial Gamma-Ray Flashes (TGFs) in sub-millisecond duration and even minute-long gamma ray glows from thunderclouds. These observations and measurements paved the way to the newly emerging field of High-Energy Atmospheric Physics [1] which deals with the production and propagation of energetic radiation, and the effects of both on atmospheric electrodynamics.

1.2. Observations, measurements and possible source mechanisms

In 1994, BATSE (Burst and Transient Source Experiment) onboard the Compton Gamma-ray Observatory, detected bursts of gamma-ray flashes generated by thunderstorms [2] and they were named TGFs (in fact, being generated by accelerating electrons, TGFs could also be considered as X-rays). TGFs are intense bursts of gamma-rays and X-rays lasting a few milliseconds or less [3]. The energy of the photons in these TGFs may extend up to about 100 MeV [4]. The only mechanism that can produce such flashes is the bremsstrahlung interaction of electrons with air. Theory has also been developed based on electron runaway mechanism to explain the production of X-rays by thunderstorms [5]. Recently, satellite observations have even observed beams of positrons emanating from thunderclouds [6].

In addition to satellite observations of TGFs, high-energetic X-ray and gamma-ray flashes have been observed to be generated by thunderclouds using both in-situ and ground-based experiments. In 2004, Dwyer et al. [7] observed a flash of gamma-rays generated by a thundercloud with photon energies as high as 10 MeV at ground level. Then in 2009, Dwyer et al. observed a TGF-like event at ground level with energy exceeding 20 MeV [8]. A different type of thundercloud generated gamma-ray or X-ray flashes, in the form

of surges, and lasting up to many seconds, have also been observed by other scientists at other geographical locations [9], [10].

For bremsstrahlung process to produce such energetic radiation, the electrons accelerated by the electric field in the atmosphere must gain relativistic speeds. If the electric field in air exceeds about 3×10^7 V/m at atmospheric pressure (this critical field decreases with decreasing pressure), the energy gain per unit length from the electric field could become more significant than the energy loss over that length. In which case, the electrons continue to accelerate, gaining increasing amounts of energy [11]. Such electrons are called runaway electrons, and this mechanism is called cold-runaway or thermal-runaway in current literature. However, with the aid of seed electrons with energies in the order of few tens of eV, even a lower electric field about 2.8×10^5 V/m is sufficient to initiate a runaway condition [12]. Runaway electrons can reach relativistic speeds and, during collisions with atoms, they can generate more relativistic electrons, giving rise to an avalanche of them [13]. When these runaway electrons collide with air, they produce X-rays. C. R. T. Wilson, the Nobel laureate, hypothesised that the runaway mechanism might take place in thunderstorms where large electric fields that are capable of generating runaway electrons exist over a vast region of space [14].

Now, after more than two decades of observations and measurements, it is a well-established fact that electrical discharges produce high energetic radiation. They are either emitted as soft X-rays of a few keV energy or X-rays and gamma-rays of several MeV energy (Moore et al. [15]; Dwyer et al. [16], [17]; Rahman et al. [18]; Nguyen et al. [19]; March and Montanyà, [20]; Kochkin et al. [21]). Experiments show that not only lightning flashes but also laboratory discharges generate X-rays (as first shown by Dwyer et al. [17]). The exact mechanism that leads to the generation of X-rays in laboratory sparks is still under investigation. It has been suggested, however, that the field enhancements caused during streamer encounters could be one possible mechanism that generates X-rays (Cooray et al. [22]). During these encounters, electrons could be accelerated beyond the threshold energies necessary for them to become runaways in the lower background fields. Recent experimental observations have supported the main idea of this hypothesis that the streamer encounters can cause X-ray emissions [21], [23]. In the case of the positive breakdown in the laboratory, X-rays indeed appear when the positive streamers from the high voltage electrode meet the negative streamer that originates from the ground electrode [21]. In recent studies, X-ray emissions were observed during the initiation of negative leaders from the high voltage electrode [24]. Even in this case, encounters occur between positive streamers originating from the space stem and the negative streamers originating from the high voltage electrodes.

2. Background, motivations, and the objectives

This chapter provides the background, motivation, and the objective for each paper included in this thesis work.

2.1. Understanding the effect of electrode geometry

As previously mentioned, X-rays have been recorded both from natural discharges in the atmosphere and from discharges in the laboratory. Many experiments have been conducted to understand the X-ray production from laboratory discharges (Dwyer et al. [17]; Rahman et al. [18]; Nguyen et al. [19]; Dwyer et al. [25]; March and Montanyà, [20], [26]; Kochkin et al. [21], [23]).

In these experiments, the detection of X-ray radiation, the region of the radiation emission in the gap, the energy and the spatial distribution of the radiation, and the stage of the discharge process from where the radiation is generating have been studied. Further, the influence of the applied voltage, the derivative of the applied voltage, the polarity and the rise-time of the applied voltage, the electrode shapes, and the gap lengths, etcetera were also studied.

The following observations concerning the electrode geometry were made in these experiments. In experiments performed by Dwyer et al. [25] with sphere-sphere, rod-sphere, and rod-plane electrode configurations, the most intense bursts of X-rays were observed when two 12-cm-diameter spherical electrodes were used. In other words, it was the larger electrode (12-cm-diameter sphere as compared to the 1-cm-diameter rod), which produced the brightest X-rays. Their observation further suggests that it was not only the electric field configuration at the high voltage electrode that was influencing the runaway electrons. As one possible reason for this observation, the higher voltage, achieved in the gap before the breakdown occurs in the case of larger electrodes, was mentioned.

In a later study, March and Montanyà [26] studied the influence of the positive and negative electrodes in the production of runaway electrons. They found that emissions were affected by the distribution of the equipotential lines around the cathode. This conclusion was based on the observation that the X-ray detection rate was increased when the grounded electrode (cathode)

was changed from the plane to the longer cylindrical electrodes in the case of positive polarity sparks. For negative polarity sparks, no such influence was observed when the grounded electrode (anode) was changed similarly.

Therefore, it is necessary to conduct more experiments in order to understand the effect of electrode geometry in X-ray production from laboratory discharges in general, and specifically the effect of anode geometry. The work described in **Paper I** is our attempt at conducting an experiment to find the effect of anode geometry in X-ray production from laboratory discharges.

2.2. The energy distribution of X-ray photons

Energy distribution of X-ray photons generated by laboratory discharges is of interest in understanding the mechanism of X-ray generation. The energy distribution of photon generated provides information concerning the maximum and average energies to which the electrons are accelerated. This information, in turn, can be used to test the predictions of the suggested mechanisms. Additionally, the energy distribution of X-ray photons itself fit into the broad spectrum of electromagnetic radiation emitted by laboratory discharges, and it fills a gap in the knowledge of such discharges. However, in practice, measuring the energy of individual photons is difficult due to various reasons. The quantification of the measured X-ray radiation in both time domain and energy domain is a difficult task mainly because of limitations in detectors.

Detection of X-ray bursts from electrical discharges is typically carried out using scintillation detectors. When an X-ray burst generated from an electrical discharge is absorbed by the scintillator crystal in an X-ray detector, these detectors produce higher output compared to individual photon energy when several X-rays photons in the burst hit the detector during the combined response-time of the measurement system and the detector.

Therefore, in order to quantify X-ray energies from electrical discharges, the scintillation detectors can be shielded using attenuating material like lead. Previously, experiments were carried out with lead-shielded detectors along with unshielded detectors in measuring X-rays produced by rocket-triggered lightning (Dwyer et al. [16]) and also laboratory discharges (Dwyer et al. [17]). Based on the responses of shielded and un-shielded detectors, these experiments also indicate that the measured energy from the unshielded detectors is higher than the individual X-ray photon energy of the associated bursts. In another study, Dwyer et al. [25] reported that the average photon energy could be around 230 keV while the total deposited energy could be as high as 50 MeV. Work carried out by Kochkin et al. in [21], [23] using attenuators reported that the characteristic X-ray photon energy of such sparks is on the order of 200 keV. In a detailed study, by assuming certain distributions for X-ray fluence and photon energy, Carlson et al. [27] reported that the experimental results of X-rays from 1 MV electrical discharges could be modelled

by an exponential X-ray distribution having a mean around 86 keV. Kochkin et al. [28] predicted that the mean energy of such sparks is 160 keV, using a Monte Carlo model for electron and photon dynamics in an experimental setup with lead attenuators.

Depending on the method of simulation or the numerical model, the results obtained from these previous experiments yield slightly different results. For example in the case of works [23], [27], [28], which are based on somewhat common experimental data, depending on the simulation strategy or the numerical model different results are obtained. This difference could be attributed to inclusion or exclusion of photon pile-up at the detector, the primary experiment parameter used in the attenuation models (registration rate vs. total detected energy) and it could also be attributed to the inclusion of many physical processes in the simulations or the numerical models. It is important to highlight that the inclusion of each physical process in a simulation comes at the cost of also involving unknown or more assumed parameters.

Motivated by these findings, the work presented in **Paper II** is our attempt at finding the X-ray energy distribution of 1m long laboratory sparks. In this work, the objective was to design an experiment using copper attenuators and use a numerical model only based on the attenuation of X-ray photons. Thus, a minimum number of unknown parameters are kept in the numerical model. Based on the proposed numerical model, it was expected to predict the probable energy distribution(s) of such 1m laboratory sparks, and also to predict the total number of X-ray photons generated from such sparks.

2.3. X-rays produced by upward initiated lightning flashes

Cloud to ground lightning flashes can be divided into three categories: Natural downward lightning, artificially triggered lightning, and upward initiated lightning. The first unambiguous observation of X-ray generation from lightning flashes was made by Moore [15], who recorded X-ray bursts associated with the stepped leaders of natural downward lightning flashes. Since then, X-ray bursts have been measured from natural cloud to ground lightning and triggered lightning in a series of experiments conducted at Camp Blanding in Florida since 2002 [16], [29], [30]. The bursts of X-rays observed at Camp Blanding appear to coincide with the stepping phase of the stepped leaders in natural lightning and the dart leader phase of both natural and triggered lightning. In a similar study carried out in Gainesville, Florida since 2010, X-rays associated with subsequent-stroke leaders were found to be more intense compared to X-rays associated with first-stroke leaders [31]. X-rays appear in bursts of the order of a microsecond, with a typical total duration of about 1 ms or less, and carry energy up to the region of MeV. On the other hand,

measurements of X-ray emissions from natural upward lightning is scanty. In a recent experiment, Montanyà et al. [32] made measurements of X-ray emissions from several upward lightning flashes from a tower located at 2500 m altitude. They could not detect X-ray emissions from the 12 upward initiated negative ground flashes.

Motivated by these facts, in 2011, we installed an X-ray detection system in close proximity to the Gaisberg Transmission Tower (GBT), which is located at a 1300 m altitude in Salzburg, Austria. This location was chosen because GBT is struck by natural upward initiated lightning several times a year. The X-ray detection system was integrated into the existing lightning characteristics measurement system at GBT. This experiment and the results are presented in **Paper III** of the thesis.

2.4. X-rays produced by switching impulses

X-ray bursts from high-voltage laboratory sparks in air were first observed by Dwyer et al. [17]. The existence of high energy radiation from lightning and especially from laboratory discharges raise questions as to the possible mechanism behind this radiation. This mechanism is likely to involve runaway electron breakdown [13]. Later many experiments were conducted [18]–[21], [23], [25]–[27], [33] in laboratory. March and Montanyà [20] reported that HV impulses with rapid rise-time tend to produce more X-rays emissions with higher energies than longer rise-time impulses. However, so far nobody has conducted measurement with much longer rise-times compared to lightning impulses. Since X-ray bursts from laboratory sparks were detected only from air gaps stressed by the lightning impulse similar to the return strokes and the mechanism of X-ray generation by laboratory sparks remains uncertain, a further study of this phenomenon is an order.

In **Paper IV**, we present results of an independent experiment where the production of X-rays was measured from an air gap stressed by switching impulses. The voltage rise-time of such switching impulses are about two orders of magnitude greater than lightning impulses.

3. Methodology

This chapter is divided into five subsections. The first section provides an overview of a typical scintillation X-ray detector setup, which is utilized in all experiments described in the four papers included in this thesis. The experimental setups related to papers (I), (III) and (IV), and the experimental setup and the numerical model used in the paper (II) are described in the remaining four sub-sections.

3.1. A typical scintillation X-ray detection system

In order to detect bursts of X-rays from transient events such as laboratory discharges or lightning with precise timing, detectors based on scintillation crystals coupled with photomultiplier tubes (PMT) are used because of their fast response compared to other types of radiation detectors. Thallium-doped sodium iodide (written as NaI(Tl)) is the most commonly used scintillation material in such X-ray detectors because of its high efficiency and lower cost. Other scintillation materials such as BaF₂, CsI, LaBr₃, are also common.

3.1.1 Principle of operation

When a single or multiple X-ray photons hits a scintillator crystal in an X-ray detector, each X-ray photon produces several visible light photons. These photons are collected by the cathode of the photomultiplier tube attached to the scintillator and are converted to an electrical current which is multiplied by each stage in the PMT and is finally produced as a voltage pulse at the anode of the PMT. NaI(Tl) has a visible-photon yield of roughly 30 to 40 photons per 1 keV of absorbed X-ray radiation. With such a photon yield, and with a typical PMT supply voltage of 1 kV, a typical NaI(Tl)-PMT detector assembly has an energy detection range from a few keV to several MeV.

3.1.2 The complete detection system

The scintillation detector systems used in all experiments in this thesis work primarily consist of four major components. These components are, one or a pair of integrated scintillator-PMT detector assemblies (NaI(Tl) scintillators in most cases), the high voltage power supplies for the PMTs, corresponding fibre-optic transmitters (which convert the electrical signal from PMT anode to an optical signal) and a 12 V battery. The 12 V battery powers both the PMT high voltage power supplies and the fibre-optic transmitters. These components are usually housed inside a completely sealed aluminium enclosure as shown in Figure 1. The only output from such an aluminium enclosure is one or more fibre-optic cables. The aluminium enclosure shields components inside from electromagnetic interference and also acts as an extra light shield (for the PMTs). This self-contained detector system housed in the aluminium enclosure can be operated in extremely noisy environments such as a high voltage laboratory and can also be operated outdoors in order to detect X-rays from lightning flashes. Such a complete detector system is sometimes simply called as an ‘X-ray detector’ in this thesis and the included papers. The optical output of such an X-ray detection system is transmitted via fibre-optic cables and is converted back to an electrical signal by a fibre-optic receiver and is recorded by a transient recorder.

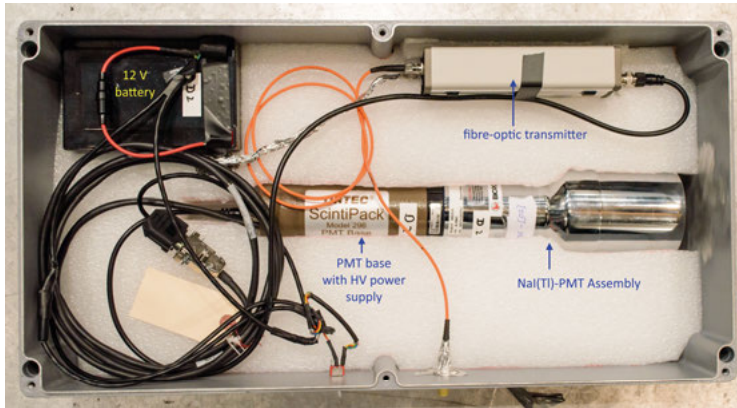


Figure 1. A typical X-ray detector system. The aluminium enclosure containing the components is photographed opened. An integrated NaI(Tl)-PMT assembly (right) is connected to the PMT-base with HV power supply (middle). The fibre-optic transmitter can be seen directly above the detector assembly. A rechargeable 12 V battery visible in top-left powers both the PMT-base and the fibre-optic transmitter.

3.1.3 Efficiency of a scintillation X-ray detector system

The efficiency of an X-ray detector system is primarily determined by the absorption efficiency of the scintillation crystal, the light yield of the scintillation crystal, the PMT gain, input range and resolution of the fibre-optic transceiver system, and finally the thickness of the aluminium enclosure of the detector system.

The scintillation could be described as the emission of a certain number of visible photons when the scintillation crystal absorbs an X-ray photon. The absorption efficiency depends on the dimensions of the scintillation crystal. For example, a cylindrical NaI(Tl) crystal of 76 mm thickness and 76 mm diameter (most commonly used in this thesis work) has a roughly 80% absorption efficiency for 1 MeV photons and almost 100% absorption efficiency for 500 keV photons. Thus, the efficiency of the detector system decreases with the energy of the X-ray photons.

The light yield of scintillator crystal, which is a measure of its sensitivity, gradually decreases over time, and this is accelerated by prolonged exposure to intense radiation. This degradation can be compensated to a certain extent by adjusting the gain of the PMT (by increasing the HV power supply of the PMT).

However, the absolute minimum detectable energy of an X-ray detector system is usually determined by the thickness of the aluminium enclosure. The detection threshold of the NaI(Tl)-PMT assembly itself is even lower. This minimum detectable energy is usually on the order of 20 to 30 keV. However, depending on the resolution of the fibre-optic transceivers and signal to noise ratio of the overall system, the minimum detectable energy could be as high as 100 keV. The maximum detectable energy is either determined by the scintillation crystal thickness, or by the input voltage range of the fibre-optic transmitters and overall gain of the scintillator-PMT assembly, and it is at least a few MeV.

3.1.4 Rise and decay times of a detector and their implications

The decay-time of NaI(Tl) scintillation crystal is roughly 250 ns, and it also usually determines the total decay-time of the complete detection system. However, the rise-time of the detection system is primarily determined by the fibre-optic transmission links because of their limited bandwidth.

Because of the implications of the rise and decay times, the X-ray detector systems are capable of resolving an X-ray spectrum correctly only if certain conditions are satisfied. When several X-rays photons in a burst hit the detector within the combined rise-time of the measurement system and the detector, these detectors produce a higher output compared to individual photon energy. The probability of such multi-photon accumulation depends on the surface area of the scintillator crystal, the distance from the source, and

the fluence of the photons (could be a few photons to tens of photons). In cases where low energetic photon(s) and high energetic photon(s) hit the detector within the decay-time, low energetic photon(s) may not be successfully detected. Because both laboratory and natural discharges in the air are known to produce bursts of X-rays, these implications are very relevant to this thesis work.

The rise and decay time of detector systems can be improved by various means. The use of slower fibre-optic links can be eliminated by keeping both detector system and transient recorders together contained in an EMC cabinet with a radiation entrance window. The power supply for the recorders should also be kept inside the EMC cabinet in this case. The other obvious method is the use of detectors with fast response time with faster fibre-optic links. BaF₂ based scintillator crystals are fast, but their light yield is lower compared to NaI(Tl). LaBr₃ or its variants based scintillators are the best choice in this regard. They are both fast, and their sensitivity is comparable to NaI(Tl) scintillators. However, the much higher cost of LaBr₃ scintillators restricts their widespread usage.

3.1.5 Calibration of X-ray detector system

The X-ray detector systems are usually calibrated on site and frequently. The calibration is carried out by placing a radioactive isotope such as ¹³⁷Cs (with very low radioactivity in order to reduce radiation exposure) emitting gamma rays directly on top of the X-ray detector and measuring the amplitude of the resulting peak by a transient recorder connected to the fibre-optic receiver. The calibration waveform also depicts the response of the detector system to a single photon event. The rise-time of the peak is mainly determined by the bandwidth of the fibre-optic link while the decay-time is equal to the decay-time of NaI(Tl) scintillation crystal.

Instead of measuring a single peak, the waveform accumulation mode of a transient recorder can be used to superimpose the detected X-ray peaks within a short time window. By using this method, peaks due to ¹³⁷Cs calibration source are intensified compared to any background radiation peaks. Figure 2 depicts such a superimposed acquisition of 662 keV photons from a ¹³⁷Cs source.

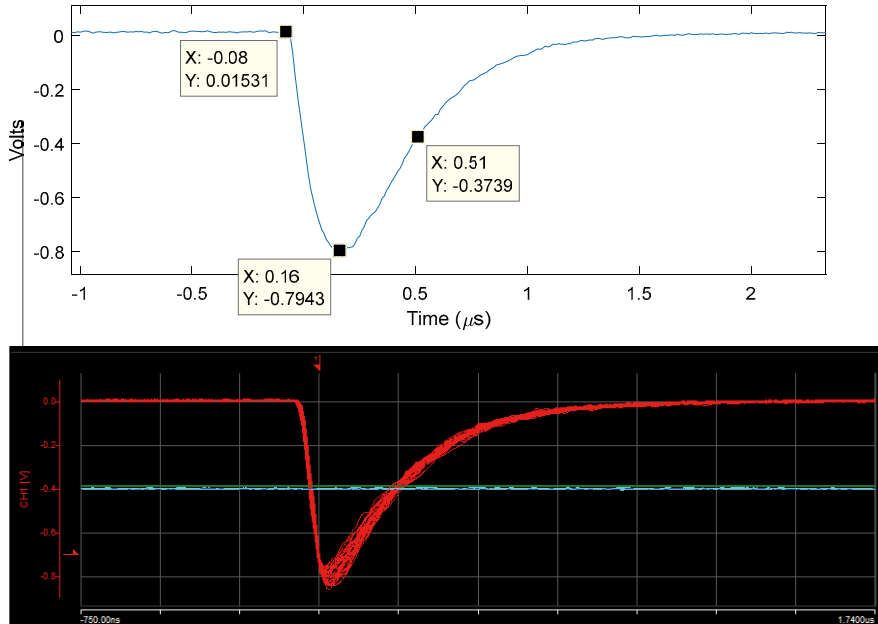


Figure 2. Calibration of X-ray detector system using a ^{137}Cs source. The upper plot shows a single record corresponding to 662 keV emission of a ^{137}Cs isotope. The lower plot shows the accumulation of photons from a 20 kBq ^{137}Cs source, placed directly on top of an X-ray detector enclosure for about 500 ms. The number of accumulations in the lower figure depends on the radioactivity of the calibration source. The prospect of using a background radiation peak as a calibration waveform could be avoided by this method. The seemingly lower rise-time as can be seen from both plots is caused by the limited bandwidth of the fibre-optic link. The fall-time of the signal is primarily due to the typical scintillation decay-time of NaI(Tl).

The calibration constant is calculated by assuming a simple linear relationship of the peak amplitude of the detected signal to the total-deposited-energy at the detector. Such calibration, based only on the amplitude, is especially applicable to NaI(Tl) detectors coupled to fibre-optic links with limited bandwidth as described next.

A calibration waveform (a single-photon-event) and the detector response to an X-ray burst of a laboratory discharge with total-accumulated-energy around 2.7 MeV are shown in Figure 3. This NaI(Tl) detector, as can be seen from the data-cursors in Figure 3, has a very similar response to the single-photon event and the multi-photon-accumulation. The energy of the multi-photon-accumulation is determined by the amplitude of the waveform using the same linear calibration constant described above. The energy determined in this way is valid under the assumption that the amplitude of the response of such a multi-photon accumulation is equal to the sum of the amplitudes corresponding to the single-photon response of each photon in the burst.

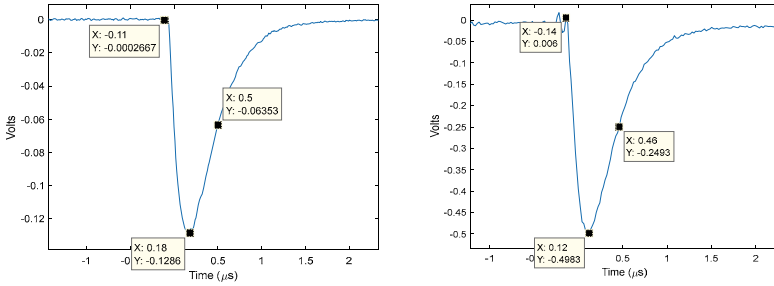


Figure 3. The response of NaI(Tl) detectors coupled to a fibre-optic link with low bandwidth. The response to a single photon emission of a ^{137}Cs calibration source (left) and the typical response to a laboratory discharge of a standard lightning impulse of 900 kV (right) are shown. This detector configuration is not capable of resolving multi-photon-pile-ups for photon bursts occurring within the response time of the system (as evident from the response to a multi-photon burst of the detector shown in the right). (Obtained from Paper III)

As discussed in Section 3.1.4, and as evident from Figure 3, the response of a typical scintillator detector setup to a multi-photon pile-up could be indistinguishable from a single photon response. This fact is also confirmed by our experience of NaI(Tl) detector response in the laboratory (Paper I and Paper II) and other independent laboratory experiments using even much faster LaBr₃ detectors [23], [27]. Based on the findings of tests conducted recently, X-ray bursts from laboratory discharges last probably a very short time in the order of a few nanoseconds or even sub-nanoseconds [28]. It will be evident soon from the results and the discussion related to Paper II, depending on the problem, we can overcome some of these implications by assuming that voltage pulses recorded from X-ray detectors are always produced by an accumulation of multiple photons at the scintillation crystal of a detector.

3.1.6 The effect of background radiation and statistical probability of false detections

At any given location (inside a laboratory or outdoors) a sufficiently long recording of the output of an X-ray detector system consists of peaks corresponding to the natural background radiation. This radiation is caused by the atmospherically scattered cosmic background radiation, the airborne radionuclides such as radon-222, the natural radioactivity of the Earth and surrounding materials etcetera. For example, a one-second exposure of a typical NaI(Tl) detector system to the background radiation provides around 50-200 detectable X-ray peaks (see Figure 4). Usually, the time windows related to the measurement of X-rays from both lightning (related to strokes and other transient events) and laboratory discharges are in microsecond scale. Therefore, the probability, which such a background radiation event is coinciding with a measurement is extremely low. This probability can further be reduced

significantly by utilising more than one X-ray detector. The possibility of two adjacent detectors detecting the same natural background radiation event is very low because the background radiation at ground level at a given location usually consists of isolated X-ray or gamma-ray photons.

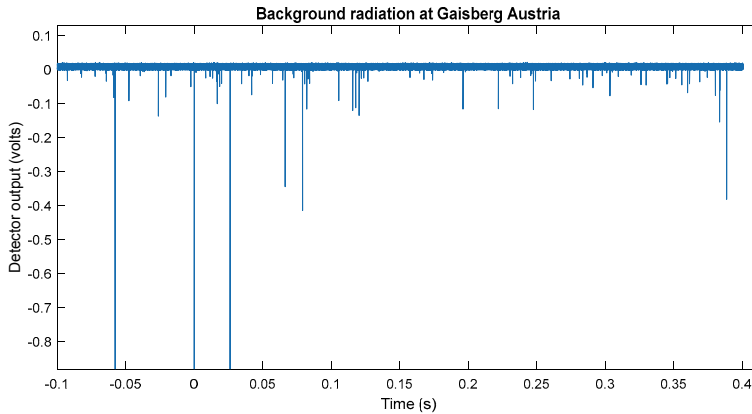


Figure 4. Background radiation peaks recorded in the vicinity of Gaisberg Tower, Austria. Record length is 500 ms. Calibration constant is roughly 4.4 keV / mV.

3.2. Influence of the anode geometry in X-ray production (Paper I)

The experimental study reported here was conducted at the high voltage laboratory of Uppsala University, Sweden with the objective of observing the effect of anode geometry in X-ray production. The experiment was designed in such a way that all other experimental configuration was kept constant while the anode geometry was changed.

3.2.1. Experimental setup

Figure 5 shows the approximate arrangement of the experiment schematically. A rod-sphere configuration was chosen as the electrodes. The rod was made of brass and had a diameter of 10 mm. Three different spheres were used with the diameters 2.1, 6.3 and 12 cm respectively. A negative standard lightning impulse voltage (the impulse front-time is 1.2 μ s, and time-to-half-value is 50 μ s) was applied to the rod. The grounded sphere in each configuration effectively served as the anode. The gap length was 95 cm. The voltage impulse was generated by using a Marx impulse voltage generator. The charging voltage of the Marx generator was 950 kV. This charging voltage which was applied to the rod-sphere air gap was enough to create a spark breakdown between the electrodes.

Spheres with three different diameters were used as the anode and for each rod-sphere combination, 15 sparks were applied. The voltage across the gap,

the current through the gap and the emission of X-rays produced by the laboratory spark were measured. More detailed description of the measurement system is given in Paper I.

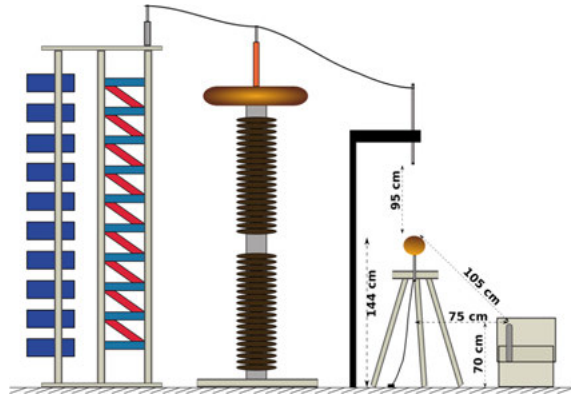


Figure 5. The experimental setup: showing (from left to right) the Marx generator, voltage divider, spark gap and the X-ray detector (not in real proportions). (Taken from Paper I).

3.3. Energy distribution of X-rays from laboratory discharges (Paper II)

The following sections briefly describe the experimental setup and the numerical model used in work described in Paper II.

3.3.1. Experimental Setup

A rod-sphere air gap was used at atmospheric pressure where the rod was made of brass and had a diameter of 10 mm. A sphere of diameter 2.1 cm was used as the anode. A negative standard lightning impulse voltage was applied to the rod. The gap length was 95 cm. The voltage impulse was generated by using a Marx impulse voltage with a charging voltage of 950 kV. The experimental setup used in this work is very much similar to the experimental setup described previously in section 3.2.1 and Figure 5 shown above is also applicable to this setup. The primary differences in this setup compared to the previous experiment are the use of an anode of fixed-diameter of 2.1 cm and the use of attenuators surrounding the X-ray detector assembly as described next.

First, a series of 15 sparks was applied where the NaI(Tl) detector was used un-shielded. Then a further 120 sparks were applied in 8 series with 15 sparks per series by covering the NaI(Tl)-PMT detector assembly with copper shields of increasing thickness. The shield, which covers the scintillator crystal of the detector entirely, was constructed by using multiple layers of a copper sheet of thickness 0.3 mm. The effective shield thickness was varied from 0.3 mm

to 2.4 mm by using a single layer up to 8 layers of copper shields in each series. A more detailed description of the complete experiment is given in Paper II.

3.3.2. Numerical model of X-ray attenuation

In order to find the source distribution of X-rays from the experiment, a numerical model was formed considering the attenuation of X-ray photons along their path from source to the NaI(Tl) detector. The average of the total-accumulated-energies of sparks in each series (with varying attenuator thickness) was compared with a numerically modelled result to achieve the goals of the experiment.

The spark is assumed to be an isotropic point source, and the differential photon intensity is denoted by function $f_0(E)$. The function $f_\Omega(E)$ is defined as the differential photon intensity at the source confined to a solid angle Ω (calculated using the distance from the detector to the source, r and the surface area of the detector, A_{det}). The function $f_\Omega(E)$ can be calculated by multiplying $f_0(E)$ by the factor $\Omega/4\pi$ as given in Equation (1).

$$f_\Omega(E) = \frac{\Omega}{4\pi} f_0(E) \quad (1)$$

The total number of photons confined to the solid angle Ω having energy from E_{\min} to E_{\max} at the source can be calculated by the integration of $f_0(E)$ with respect to energy,

$$N_{Ph(s)} = \int_{E_{\min}}^{E_{\max}} f_\Omega(E) dE \quad (2)$$

moreover, the total energy of the photons at the source confined to the solid angle Ω is given by the integration,

$$E_{total(s)} = \int_{E_{\min}}^{E_{\max}} E f_\Omega(E) dE \quad (3)$$

The total detected energy by the NaI(Tl) X-ray detector is calculated by considering the attenuation from the air, aluminium enclosure, which is 3.1 mm thick, and the copper shield of varying thicknesses.

For a given intensity I_0 , the attenuation of monoenergetic photons due to a mass of a particular material with thickness x , density ρ , and attenuation coefficient μ is given by,

$$I = I_0 e^{-(\mu/\rho)x} \quad (4)$$

where I is the intensity after the attenuation, and the term (μ/ρ) , which is dependent on the energy, is called the mass attenuation coefficient of the material considered for a given energy E .

The total detected energy by the detector can be calculated by combining equations (3) and (4) (assuming a 100% absorption efficiency) and given is given by,

$$E_{total(det)} = \int_{E_{min}}^{E_{max}} e^{-(\mu/\rho)_{Cu} x_{Cu}} e^{-(\mu/\rho)_{Al} x_{Al}} e^{-(\mu/\rho)_{Air} x_{Air}} E f_{\Omega}(E) dE \quad (5)$$

Additionally, the total number of photons detected is given by,

$$N_{ph(det)} = \int_{E_{min}}^{E_{max}} e^{-(\mu/\rho)_{Cu} x_{Cu}} e^{-(\mu/\rho)_{Al} x_{Al}} e^{-(\mu/\rho)_{Air} x_{Air}} f_{\Omega}(E) dE \quad (6)$$

NIST X-ray mass attenuation coefficient database, NISTIR 5632 [34], is used to find the mass attenuation coefficients, (μ/ρ) for air, copper, and aluminium for varying X-ray energies. Because (μ/ρ) is energy dependent and given in tabular format, the integrations in Equations (5) and (6) could only be solved numerically (even when an analytical expression for $f_0(E)$ is known).

If analytical probability density function (or a differential intensity function) governing the photon spectrum is assumed to be $S(E)$, the function $f_0(E)$, governing the spectrum and number of photons at the source can be calculated directly by multiplying $S(E)$ by a constant of proportionality k_s .

$$f_0(E) = k_s S(E) \quad (7)$$

By comparing the modelled result of equation (5) for a given distribution function $S(E)$ with experimental results, the distribution parameters of the function $S(E)$, its validity, the total number of photons emitted at the source, and the number of photons reaching the detector can be found.

3.4. X-rays produced by upward initiated lightning (Paper III)

This section describes the experimental work carried out to measure X-ray emissions associated with upward initiated lightning from 100 m tall Gaisberg Transmission Tower (GBT) at the small mountaintop called Gaisberg (1287 m above sea level) in Salzburg, Austria.

3.4.1. Experimental setup

X-ray detector was located at a distance of 200 m from the top of the GBT on the rooftop of a structure surrounding a shielded EMC cabinet (containing measurement equipment) as seen in Figure 6, and was integrated with Austrian Lightning Detection & Information System (ALDIS). The X-ray detector contained two NaI(Tl)-PMT assemblies. One was covered by a lead attenuator of thickness 2 mm, and the other was unshielded. They were housed inside an aluminium box of thickness 3.1 mm. Two fibre-optic links carried the detector signals to a transient recorder inside the EMC cabinet.

The lightning current, measured by a shunt located at the air terminal on top of GBT, was primarily used together with the X-ray detection system to correlate X-ray bursts with lightning activity.

The experiment was carried out in two phases conducted from May 2011 to July 2012 and from December 2014 to May 2015. The minimum detectable energy threshold of the second phase was improved by using a transient recorder with higher resolution and also improving the noise immunity of the X-ray detector system.

In addition to the current measurement at GBT, in some cases, the vertical electric field measured by a fast flat-plate antenna was also used in this study. More detailed information about the experimental setup is given in Paper III.



Figure 6. Gaisberg Tower and the X-ray measurement system are shown in the picture. In addition to the white X-ray detector enclosure, vertical E-field antenna, field-mill, and other meteorological instruments are located on the roof of the structure as can be seen in the red-bordered image in bottom-right. The EMC cabinet containing the measuring equipment is inside this structure. The shunts, measuring the current are placed at the tower top.

3.5. X-rays produced by switching impulses (Paper IV)

The following text briefly describes the experimental setup related to Paper IV, where the objective of the experiment was to study the X-ray produced by standard switching impulses for the first time. This short duration experiment was carried out at the high voltage laboratory at Uppsala University, Sweden during spring 2007. The experiment immediately followed the experiments with standard lightning impulses described in [25] at the same facility and contained a lesser number of sparks because of time constraints. For a more detailed description of the experiment, please refer to Paper IV.

3.5.1. Experimental setup

A Marx impulse voltage generator was configured to deliver the standard switching impulse voltage (250/2500 μ s). Two short gap lengths of 35 and 46 cm were used in this study. Then negative impulse voltages were applied (high voltage electrode negative) to different electrode configurations with the other electrode grounded. The charging voltage was set to 800 kV for all measurements. In the series of experiments with lightning impulses, it was found that the most intense bursts of X-rays were observed when two 12-cm-diameter spherical electrodes were used [25]. Furthermore, it was found that the radiation both in terms of amplitude and time of appearance were different depending on horizontal or vertical air gap. These observations motivated the use of horizontal and vertical air gaps together with big spherical electrodes. Different electrode configurations used in these experiments were as follows.

1. A sphere-to-sphere horizontal air gap of 35 cm length with both electrodes being about 120 cm above the ground (as shown in Figure 7)
2. A sphere-to-sphere vertical air gap of 35 cm length with the high voltage electrode suspended above the grounded electrode (Similar to Figure 7 but the gap is vertical)
3. A rod-plane vertical air gap of 35 and 46 cm lengths with the high voltage electrode suspended above the grounded electrode. (as shown in Figure 8)

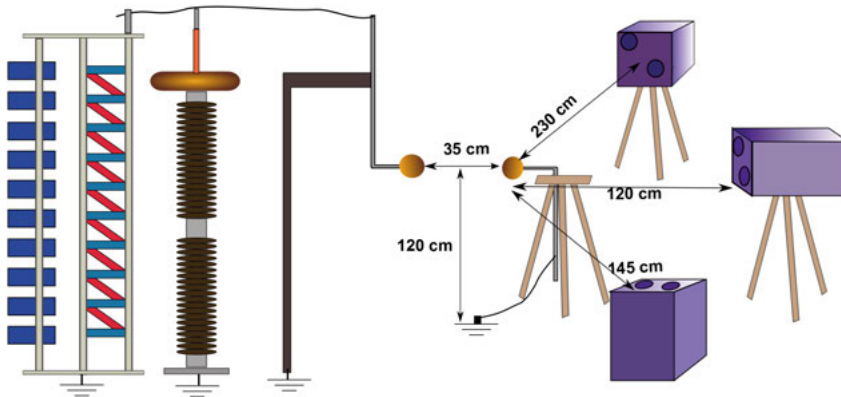


Figure 7. Schematic of the experimental setup, showing the approximate arrangement, from left to right, of the Marx generator, high-voltage divider, the sphere-to-sphere horizontal air gap of 35 cm length, and three X-ray instruments. The locations of the X-ray instruments are shown relative to the grounded electrode. The circles on the X-ray instrument boxes represent the detector-locations inside the boxes.

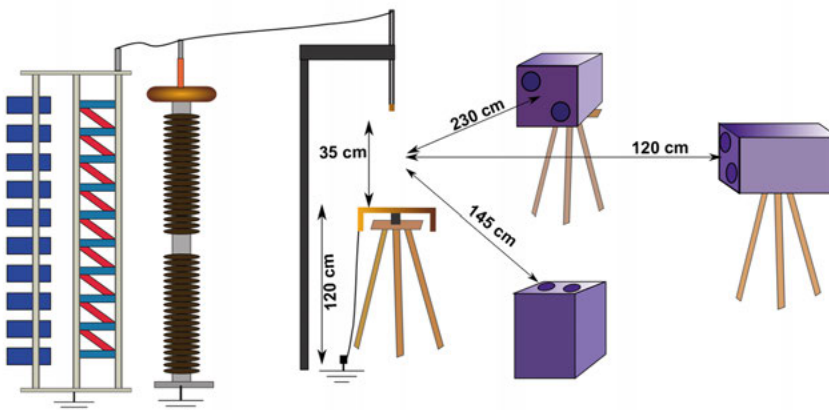


Figure 8. Schematic of the experimental setup, showing the approximate arrangement, from left to right, of the Marx generator, High-Voltage divider, the rod-to-plane vertical air gap of 35 cm length (the plane is grounded), and three X-ray instruments. The locations of the X-ray instruments are shown relative to the middle of the vertical air gap. The circles on the X-ray instrument boxes represent the detector-locations inside the boxes.

The voltage across the gap and the discharge current flowing to the ground electrode was also measured using a capacitive impulse voltage divider and a current transformer respectively.

Each instrument which measured X-rays contained two detectors. Instruments 1 and 2 each contained two 7.6 cm x 7.6 cm cylindrical NaI(Tl)/PMT detector assemblies. Instrument 3 contained one NaI(Tl)/PMT detector assembly and one (much faster response, but with lower sensitivity) plastic scintillator (36 cm x 25 cm x 1 cm) assembly.

Internal 12 V batteries powered the instruments. FM, analogue fibre-optic links were used to transmit the signals from the PMT anodes directly to the data acquisition system located in a separate, shielded room in the High-Voltage Laboratory. As a result, the detectors were very well shielded from RF noise and light leaks. The aluminium box lids allowed X-rays with energies down to about 30 keV to enter from all directions. Two of the NaI detectors were mounted inside 0.32 cm thick lead tubes that extended 4.5 cm above the top of the scintillators and also extended 41 cm below the scintillator, completely covering the PMT and the base.

Signals from all six detectors plus a measurement of the electrical current were recorded simultaneously by a transient recorder with 12-bit resolution. Also, voltages and currents were recorded separately with an 8 ns time resolution.

4. Results and Discussions

The results of the four experimental studies related to Papers I to IV are presented and discussed in this chapter.

4.1. What is the role of the grounded anode? (Paper I)

As stated before in section 3.2, in order to study the influence of anode in X-ray production, three different electrode geometries were used; where the cathode was always the same but the anode diameter was changed. X-rays were observed from 42 out of the total 45 negative sparks. Figure 9 shows the measured X-ray signal together with the voltage and the current as an example. For all sparks where X-rays were detected, X-rays occurred around 200 ns to 300 ns before the current peak. There is already a small current from anode present at this point.

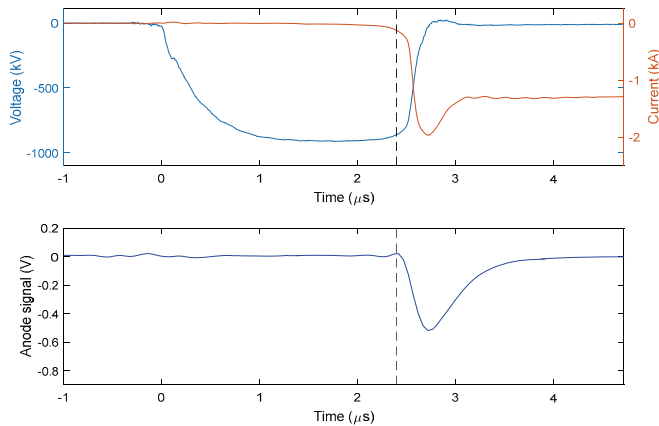


Figure 9. X-ray signal (lower) together with the voltage and the current (upper) observed from a spark for the 6.3 cm anode sphere. The pulse shape of the X-ray signal is determined by the limited bandwidth of the fibre optic link and decay-time of the NaI(Tl) scintillator. The vertical cursor is placed to indicate the occurrence of X-rays which happen around 250 ns before the peak of the current. (Figure is obtained from Paper I)

4.1.1. Energetic X-rays produced with a smaller anode

The average of the total deposited energy of the X-rays produced in each configuration is tabulated in Table 1. The average breakdown voltage and average peak current are also given.

Table 1. *Average of the total deposited energy of the X-rays detected for negative sparks together with the average breakdown voltage and current (for the 15 sparks applied in each configuration). When calculating the average, for the sparks where no X-ray signal is observed, total deposited energy is assumed to be zero.*

Anode Diameter (cm)	Average Breakdown voltage (kV)	Average peak Current (kA)	Average of the total deposited X-ray Energy (keV)	Minimum (keV)	Maximum (keV)	Standard deviation (keV)
2.1	904.6	2.66	1820	533	3189	888
6.3	915.6	2.67	1608	0	4170	1278
12.0	919.9	2.65	759	0	2330	738

As can be seen in Table 1, the average of the total deposited X-ray energy is decreasing as the diameter of the anode is increasing while the peak current and the breakdown voltage is remaining almost the same. Because all the other experimental parameters were kept constant except the size of the anode, this change of the average detected energy could only be attributed to the influence of anode geometry.

The result obtained in this experiment shows that anode geometry can also influence the X-ray production where March and Montanyà [26] did not observe a significant influence when the grounded anode was changed. According to this experiment when all other electrical and physical parameters are being constant (or fairly equivalent), the smaller the anode sphere, the higher the energy of X-rays produced.

4.1.2. Does streamer encounter produce X-rays?

The results obtained here could be explained by the theory of Cooray et al. [22], which predicts the generation of X-ray caused by negative and positive streamer encounter. A smaller anode sphere makes the longer positive streamers, and streamer encounter happens farther away from the anode. Thus, the runaway electrons produced at the meeting point can be accelerated a longer distance towards the anode and which in turn could provide more energetic X-ray photons by bremsstrahlung process. Moreover, longer streamer may carry larger charges at their heads increasing the probability of X-ray emission. In all sparks where X-rays were detected about 250 ns before the onset of the breakdown current (see Figure 9). It is also evident that there is a small current present from the grounded anode at this time. The voltage at the HV cathode

is still close to the crest. The encounter of opposite polarity streamer heads is very likely to happen at this particular time just before breakdown.

It however is, important to mention, that during previous experiments conducted at the same facility and also in other experiments [18], [23], [25] X-ray were also produced when the voltage is still rising and much prior to the time of breakdown.

4.2. What are the probable X-ray energy distributions? (Paper II)

The objective of the Paper II is the prediction of the probable energy distribution of X-rays produced by 1m laboratory discharges from negative lightning impulses, estimation of the distribution parameters and additionally the estimation of the total number X-rays photons emitted in 4π sterad from such sparks. Compared to previous studies, it was expected to use a numerical model (which was described in section 3.3 and also in detail in Paper II) based only on photon attenuation in this study. It is also important to emphasise the use of the average energy (experimentally found) in the numerical model; which in turn helps to exclude certain parameters from the model and also helps to overcome the slow response of NaI(Tl) detectors as pointed out later in the text.

4.2.1. Average energy vs. attenuator thickness

The resulting waveforms of voltage, current and X-ray are very similar to what has been described in our previous work in Paper I. The measurement system was not saturated in any of the 135 sparks. Statistics of the X-ray detector output for the total nine series of 135 sparks are tabulated in Table 2 (showing the average, maximum and standard deviation of total detected energy in each series of 15 sparks). Additionally, the number of zero energy detections out of the total 15 sparks in each series is given. When calculating the average of the total detected energy, cases where no X-rays were detected were included in the sample as a zero-energy-detection.

Table 2. *Average, maximum, standard deviation and zero detections of X-ray energy vs. Cu Shield thickness: The average is taken from each series consisting of 15 sparks with the given copper shield thickness surrounding the NaI(Tl) X-ray detector.*

Thickness of Cu Shield (mm)	0.0	0.3	0.6	0.9	1.2	1.5	1.8	2.1	2.4
Average X-ray energy (keV)	1085	1110	769	762	466	413	360	380	279
Maximum energy (keV)	3321	3662	2754	2294	1038	1238	1007	1354	734
Standard deviation (keV)	844	862	772	627	356	441	254	353	231
No. of zero detections	1	1	2	1	4	6	2	3	4

The average of the total energy detected in each series is plotted against copper thickness in Figure 10. The average energy data in above Table 2 could be fitted to a curve of first-order exponential form with a tendency to show higher copper shield thickness reducing the average of the total detected energy as expected.

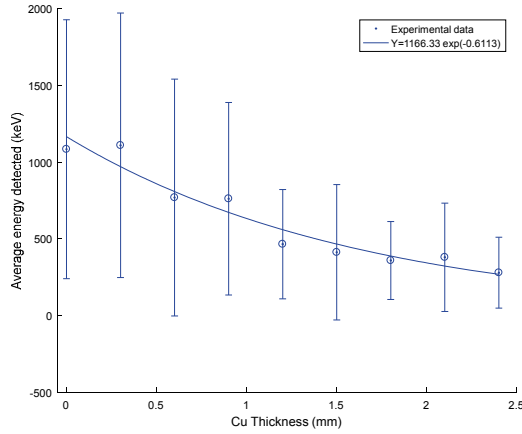


Figure 10. Experimental results of the average total detected energy fitted to a first order exponential curve. The error bars indicate the standard deviation of each data point. The fit parameters are shown in the legend. (obtained from Paper II)

4.2.2. Probable energy distributions

In order to implement the model described in section 3.3.2 a probable energy spectrum for photons is assumed first. Two such spectrums for photons are considered in this study. The first is a bremsstrahlung spectrum, in its simplest and most crude form as given by Kramers' law with unknown maximum energy. The second is an exponential photon distribution with unknown mean energy. The selection of these distributions is justified not because of any theoretical or experimental evidence of their validity but simply because they provide a rough approximation of an X-ray photon distribution for a bremsstrahlung process.

For both cases, the unknown parameters, the number of photons at the source and at the detector, the total energy produced at the source, and the total energy absorbed by the detector could be calculated. In addition to these probable photon distributions, an extreme case of a burst of monoenergetic photons is also considered as $f_0(E)$ for comparison purposes.

4.2.3. Kramers' law as a distribution

$f_{\Omega}(E)$, defined in section 3.3.2 for the case of Kramers' law, $f_{\Omega[\text{Kram}]}(E)$ can be written using Equations (1) and (7) as,

$$f_{\Omega[\text{Kram}]}(E) = k_{[\text{Kram}]} Z (E_{\text{max}} - E) / E \quad (8)$$

where the parameter $k_{[\text{Kram}]}$ is the product of the geometric distribution factor and other constants. The output of the numerical model from equation (5) is matched with experimental results by varying the two unknown parameters $k_{[\text{Kram}]}$ and E_{max} . Numerical integrations are calculated using the trapezoidal rule with an energy step size of 0.1 keV. The minimum energy E_{min} necessary to calculate the integration in (5) is considered to be 5 keV. By also employing a simple sensitivity analysis the unique and best possible values for the parameters are found to be $E_{\text{max}} = 204$ keV and $k_{[\text{Kram}]} = 0.0146$.

The resultant attenuated intensity of photons along their path is shown in Figures 11 considering the attenuation of air, aluminium, and copper. The total number of photons depicted in the figure is calculated by rounding off the integrated results to a whole number. The final simulated results, assuming 100% efficient detection, and the experimental results are shown in Figure 12.

4.2.4. Exponential distribution

Because of the somewhat arbitrary choice of Kramers' rule for photon distribution used above, there could also be other distributions which provide results in agreement with the experimental data. Therefore, an exponential energy distribution is also considered. Use of an exponential distribution is further relevant because previous statistical models used by Carlson et al. [27] and Kochkin et al. [23], [28] have also assumed exponential photon energy distributions.

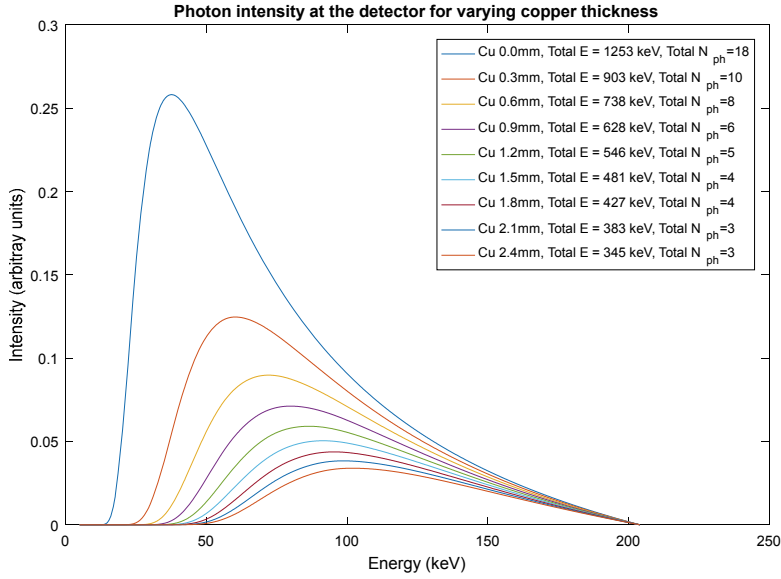


Figure 11. Simulated X-ray photon intensities confined to a solid angle Ω after the attenuation of air, aluminium box and copper shields with varying thicknesses under a Kramers' distribution. The total integrated energy and the total number of photons are also given in the legend for different Cu shield thicknesses. (Obtained from Paper II)

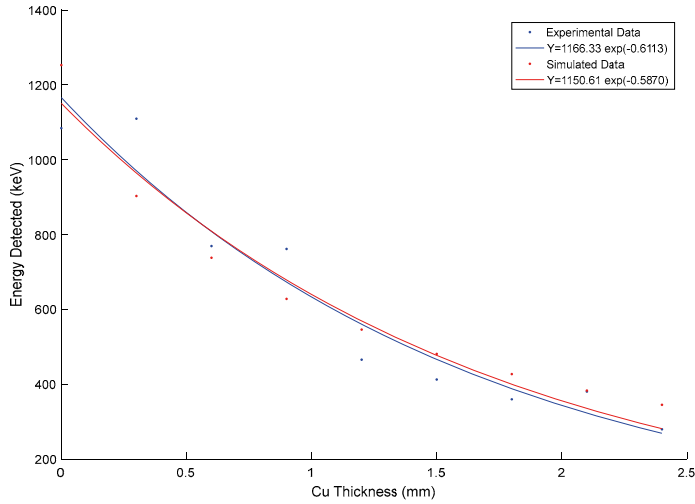


Figure 12. Simulated vs. experimental results for a photon distribution governed by Kramers' law. Both curves for experimental and simulated results are fitted to a first-order exponential curve with fit parameters shown in the legend. (Obtained from Paper II)

By using a similar approach as before, the differential intensity of X-rays photons at any given energy E confined to a solid angle Ω , $f_{\Omega[\text{exp}]}(E)$ for an exponential distribution can be defined as,

$$f_{\Omega[\text{exp}]}(E) = k_{[\text{exp}]} \frac{1}{E_{\text{mean}}} e^{-E/E_{\text{mean}}} \quad (9)$$

where E_{mean} is the mean energy of the photon distribution and $k_{[\text{exp}]}$ is defined as the product of the geometric distribution factor and the coefficient of proportionality of the distribution.

By substituting $f_{\Omega[\text{exp}]}(E)$ for $f_{\Omega}(E)$ in equation (5) and utilising the same approach as used previously for Kramers' distribution, possible combinations of values for the unknown parameters $k_{[\text{exp}]} = 47.5$ and $E_{\text{mean}} = 39.5$ keV are obtained.

The resultant photon intensities for varying copper thicknesses and the final comparison of experimental and simulated results are shown in Figures 13 and 14 respectively. The integration is carried out with a maximum energy of 950 keV (derived from the supply voltage across the gap, and assumed to be the theoretical maximum energy of photons), minimum energy of 5 keV and a step size of 0.1 keV.

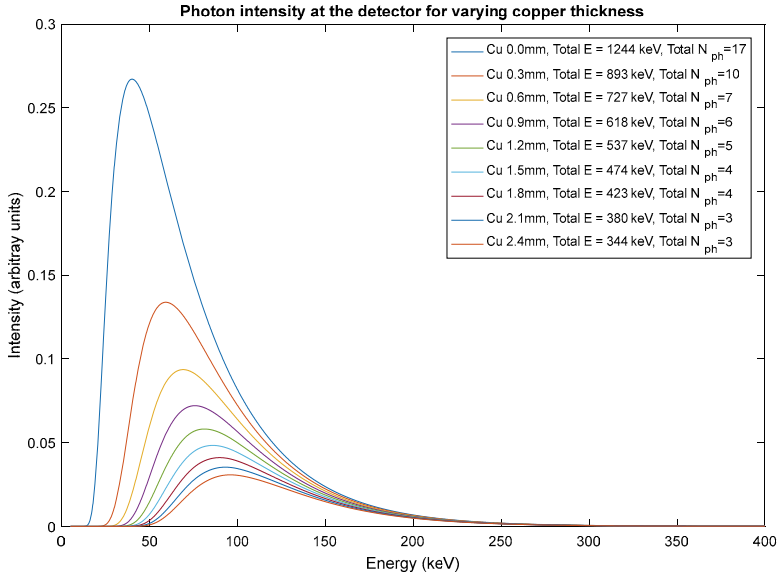


Figure 13. Simulated X-ray photon intensities, confined to a solid angle Ω after the attenuation of air, aluminium box and copper shields with varying thicknesses for an exponential photon distribution. The total integrated energy and the total number of photons are also given in the legend for different Cu shield thicknesses. (Obtained from Paper II)

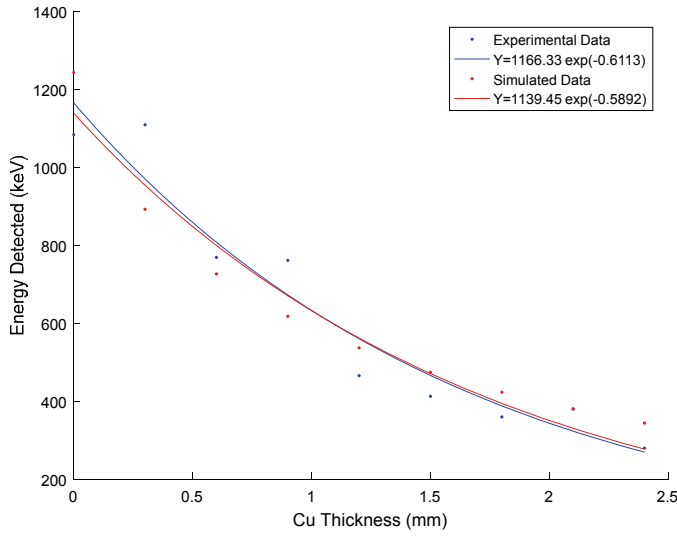


Figure 14. Simulated vs. experimental results for an exponential photon distribution. Both curves for experimental and simulated results are fitted to a first-order exponential curve with fit parameters shown in the legend. (Obtained from Paper II)

4.2.5. Comparison of distributions and concluding remarks

The mean energy of the photons under Kramers' rule and the exponential photon energy distribution is found using Equations (2) and (3). The total number photons generated at the source is found using equations (1). The mean energies of detectable photons under Kramers' distribution and exponential distribution, assuming a minimum threshold of 15 keV, are 52 keV and 54.5 keV respectively. The total number of detectable photons generated from the spark under Kramers' and exponential distributions in 4π sterad is 1.76×10^5 and 1.7×10^5 respectively. According to Figure 13, the maximum energy under an exponential distribution is about 250 keV which is not much higher than 204 keV maximum energy under Kramers' distribution. From these results, it can be concluded that both distributions yield comparable results.

The X-ray fluence has a particular distribution caused by both different luminosity of the photon bursts at the source and also by the possible non-isotropic beaming of photons as evidenced by the high standard deviation of experimental results. The energy spectrum parameters are also distributed in reality. In this study, because the distribution of photon energy is the primary concern, we have chosen to model only the energy spectrum of photons with unknown distribution parameters. The exclusion of distributions of fluence and detector efficiency from the numerical model makes it possible to conduct a more meaningful comparison of modelled results and experimental data, with fewer unknown parameters.

This exclusion is further justified by the fact that, taking the average of the total detected energy of a series of sparks experimentally, the effect of those unknown distributions is implicitly included in the averaged result. Also, the use of the average of total detected energy in the model makes it possible to assume that all detected peaks are an accumulation of multiple photons in the NaI(Tl) scintillator. Therefore, the modelled result is not sensitive to the implications of multi-photon counts due to slower response of NaI(Tl) scintillators.

4.3. X-rays observation at Gaisberg Tower (Paper III)

The result from the experimental work from Paper III is presented and discussed here. In order to determine whether a ground level detection of X-rays is associated with lightning, following identification criteria were considered.

- X-ray peaks within few hundreds of microseconds before a tower recorded RS (always utilised)
- X-ray peaks correlated to stepped, dart, or dart-stepped leader process from E-field signatures (not utilised in some cases due to lack of E-field data)
- X-ray peak(s) coinciding with different types of non-RS current peaks (always utilised)
- X-ray burst, with multiple consecutive peaks, but not coinciding with E-field or current peaks.

4.3.1. Results of the experiment

The results of the experiment which was carried out in two phases from 2011 until 2015 are presented here.

4.3.1.1. Phase 1 (May 2011 to July 2012)

During this phase, a total of 85 flashes were recorded and current measurements were available from GBT database at ALDIS. There was only one flash identified as a downward flash. Out of the remaining 84 flashes, 65 flashes were of the type of initial continuing current (ICC) without return strokes, called ICC_{Only}. 19 flashes were of the type ICC pulses followed by return strokes (RS), called ICC_{RS}. There was a total of 79 negative flashes (including the one downward flash recorded), four bipolar flashes, and two positive flashes. The classification of the type of flashes, strokes, and current pulses used above is discussed in more detail in [35], [36].

These total 85 flashes recorded contained a total of 389 pulses or strokes. The 19 flashes with RS (all negative) contained a total of 79 RS pulses. There were no X-ray detections associated with any of these ICC pulses, RS pulses

or M-component pulses (i.e., X-ray peaks within about a hundred microseconds before a pulse). It is important to mention that the signal to noise ratio of the X-ray detector system during phase 1 was lower compared to phase 2.

Even though we could not detect any X-ray bursts directly associated with a RS or any other current pulse from the 85 flashes directly struck the GBT, there was one interesting case where an X-ray burst recorded by both un-attenuated and attenuated detectors related to a close by negative downward lightning. The information about this event and its waveforms are presented in Paper III in more detail.

4.3.1.2. Phase 2 (December 2014 to May 2015)

The phase 2 of the experiment was started primarily with modification to the X-ray detector by improving the detector signal to noise ratio where X-ray peaks higher than 20 keV could be detected (which was very close to the sensitivity of the detector).

Out of these 23 flashes recorded in this phase, 9 were ICC_{Only}, and 14 were of the type ICC_{RS}. 21 flashes were negative polarity while two were bipolar. These flashes contained a total 278 pulses/strokes. The 14 flashes with RS (all negative) contained a total of 76 RSs.

X-rays were detected for the first time in three flashes which could be associated with the dart or dart-stepped leader process (X-ray peaks detected before the RS). However, both the fluence and the amplitude of the X-ray peaks were much smaller compared to previous X-ray detection from natural or rocket-triggered lightning. The detected peaks were not typical x-ray bursts, but single or two peaks, with an energy of few tens of keV to about 700 keV. Furthermore, X-rays were only detected in the un-attenuated detector, implying that the detected X-rays had lower energy compared to the accumulated energy. One such example detection is shown Figure 15.

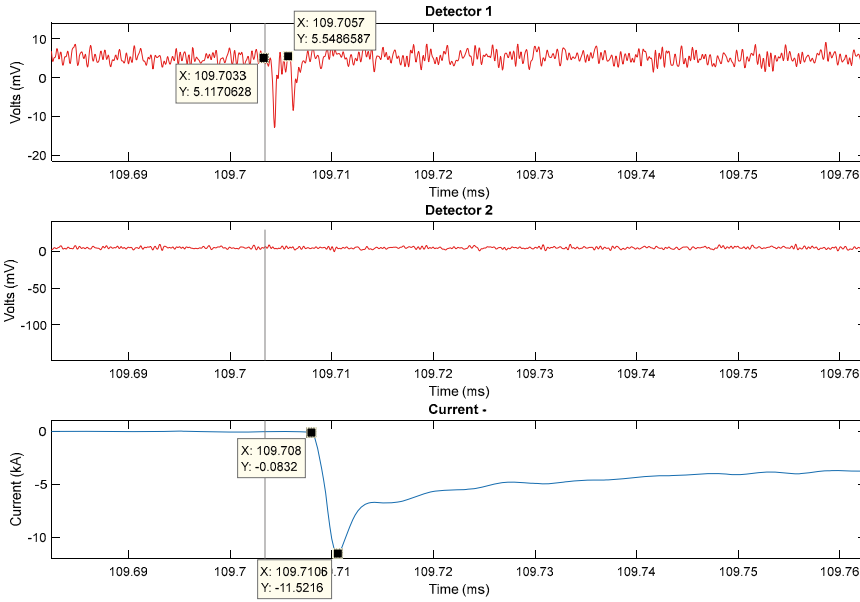


Figure 15. X-rays from a subsequent stroke of another flash occurred on 2015-03-02. Two distinct X-ray peaks are visible in the un-attenuated detector. The occurrence of first and second X-ray pulses are about 4.7 and 2.3 μ s before the onset of the current peak of the only RS. The vertical cursor is fixed at the first X-ray peak. The flash contained 17 ICC pulses before this RS. Peak energy of the burst is around 70 keV (calculated by multiplying peak voltage by the calibration factor). Timestamp of RS is 20:56:29.9889 UTC. (Obtained from Paper III)

In all three cases, X-rays occurred few microseconds before the current peaks associated to return strokes. The hundreds of ICC pulses and few M-component type current peaks did not produce any X-rays. This is an indicator that the detected X-ray peaks are associated with the return strokes and are not random events occurred due to background radiation. Also, there was no evidence of intense gamma-ray bursts with cloud origin.

4.3.2. What are the reasons for the week X-ray production?

Over a span of about ten years, X-ray emissions from triggered lightning and natural lightning have been measured successfully [16], [29]–[31]. In the case of triggered lightning, the X-ray emissions are produced by the dart and dart stepped leaders associated with the upward initiated negative ground flashes. At the beginning of the X-ray emissions, the tips of dart leaders or dart stepped leaders are located at a height of about 1 km from the ground [16], [29], [30].

However, the results presented in Paper III show that the x-ray emissions from dart and dart-stepped leaders from upward initiated lightning flashes from Gaisberg Tower are either very week or very rare.

We can rule out the possibility that the X-ray emissions are weak because the distance to the source of emission is larger than the cases studied in Florida based on the arguments presented in depth in Section 4 of Paper III. Another probable reason for the lower X-ray production could be the preconditioning of the leader channel from long continuing currents. However, similar continuing currents also exist in triggered lightning.

On the other hand, the maximum extension of the dart leaders associated with upward lightning from Gaisberg Tower is no longer than 2 – 3 km. Because of this lower extension of dart-leaders, the charge accumulated at the tip of dart leaders striking Gaisberg Tower is significantly lower than the charge that is accumulated at the end of dart leaders in the case of triggered lightning. This could be a reason for insignificant x-ray emissions from dart and dart-stepped leaders striking the Gaisberg Tower. The fact that the few X-ray emissions we have observed from lightning flashes striking the Gaisberg Tower took place just before the return stroke when the dart leader has extended to its maximum value and when the accumulated charge at its tip is at its maximum value is an indication of this.

However, more theoretical and experimental data, especially from towers located at sea level, and also from high altitude are needed to make a firm conclusion concerning the x-ray emissions from upward lightning.

4.4. X-rays produced by switching impulses (Paper IV)

The results obtained from the experimental work with the objective of recording X-rays produced by switching impulses in Paper IV are summarized in this section. As mentioned before in Section 3.5.1 three different series of experiments were performed with different electrode configurations.

4.4.1. X-rays produced by horizontal sphere-sphere gap

15 negative switching impulse voltages were applied in this configuration. In 11 cases out of these 15 applied voltages X-rays were detected in one or several of the detectors. The average breakdown voltage was around 530 kV for this series. A typical X-ray record is shown in Figure 16 (with an expanded time scale) where signals from all six detectors are shown together with the voltage and the current measurements. The placement of the detectors and their assignment to the channels in the oscilloscope are described in detail in Paper IV. The peak voltage and the peak current were about 540 kV and 1.4 kA respectively. As is evident from the waveforms, the X-rays appear at around 77 μ s after the application of the switching impulse voltage but on

average $0.74 \mu\text{s}$ before the final breakdown. Moreover, at the time of the appearance of the X-rays signals, the voltage, and the corresponding current signals started decreasing and multiple oscillations on the current signals were also visible. The total deposited energy varied from 180 keV up to the saturated peak of 6 MeV. It is important to mention that some detectors were saturated from the produced X-rays.

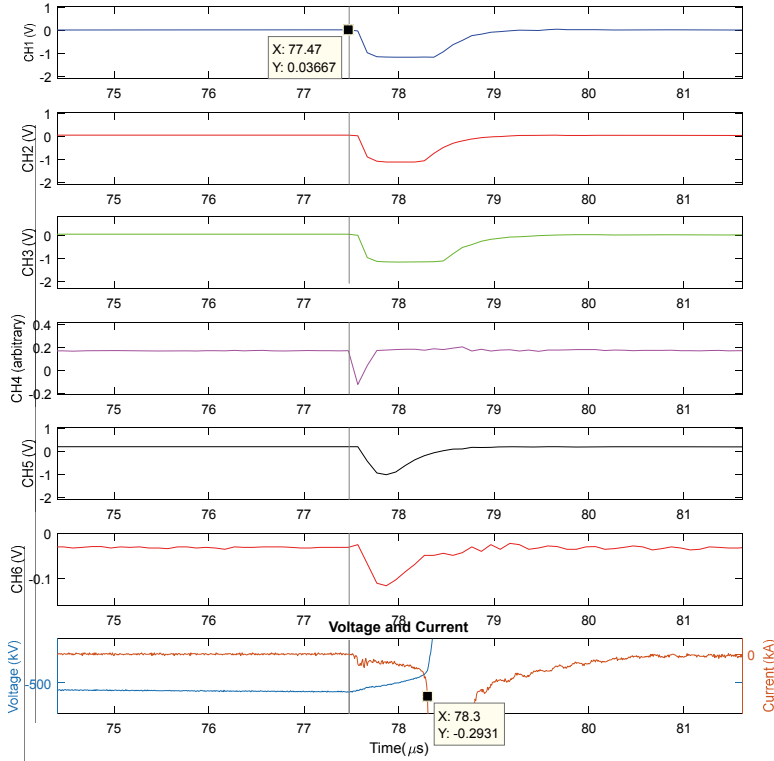


Figure 16. X-rays signals from all six detectors placed in 3 boxes together with the measured voltage and current waveforms in an expanded time scale. The voltage impulse starts at the time $t = 0$. The complete unexpanded waveform is also presented in Paper IV. The black vertical cursor placed on the plots represent the time of X-ray occurrence. At this point in time, a small current can be seen from the ground electrode, and the voltage has just started to collapse. The X-ray occurrence happens on average $0.74 \mu\text{s}$ before the breakdown. (Obtained from Paper IV)

4.4.2. X-rays produced by vertical sphere-sphere gap

For the same electrode configuration (sphere-to-sphere) and the gap length (35 cm) as described above, the second series of measurements were conducted with a vertical gap instead of the horizontal gap used previously. The grounded spherical electrode was placed on a wooden stool about 120 cm above the floor of the High-Voltage Laboratory. Again about 15 negative switching impulse voltages were applied and now in 8 cases of 15 X-rays were recorded in one or more detectors. The breakdown voltage was around 528 kV for this series. The total deposited energy varied from 150 keV up to the saturated peak of 5 MeV. All observations related to the timing of X-ray occurrence were the same as in the case of horizontal gap described above.

4.4.3. X-rays produced by vertical rod-plane gap

Then in the third series of measurements, the electrode configuration was changed to rod-to-plane as can be seen in Figure 8. In this configuration, the gap lengths were 35 and 46 cm. The breakdown voltage was around 470 and 540 kV respectively. Seven impulses were applied in the 35-cm long gap, and eight impulses were applied in the 46-cm long gap. Out of 15 applied switching impulse voltages only in one case (35-cm gap) X-rays were detected in three detectors where the energies varied from 120 keV to 490 keV. The timing of The X-rays was similar to the sphere-sphere configurations described above.

4.4.4. The origin of X-rays and comparison to X-ray production from lightning impulses

A close look at resulting waveforms from switching impulses indicates that X-rays are created either when the streamer/leader tip almost reached the opposite electrode or at the meeting point of countering streamer/leader heads a bit away from the opposite electrode. From available waveforms of voltage and current, it is not possible to accurately define whether the breakdowns are only based on streamers as in the case for breakdowns from lightning impulses with comparable gaps lengths or whether leaders are also developed. A rough estimate of the E-field enhancement at the 12 cm diameter spheres implies that the first streamer inception at the HV end should happen around 300 kV. Which in turn, according to the voltage and current waveforms, indicates that the breakdown happens around 30 to 40 μ s later from the first streamer inception. Without fine current measurements at the high voltage end, or without high-speed photographic evidence, it is not possible to find the occurrence of first streamer burst and the total time of streamer or leader propagation. However, because of the slow rise-time of the switching impulse, it is reasonable to assume that streamers generated from a switching impulse may not advance

all the way across the gap during the first inception. It is possible that several streamer inceptions had to take place before the streamers could extend all the way to the grounded electrode or encounter an opposite polarity streamer. More experiments with larger samples, including fine HV-current measurements and high-speed videography, are required to study X-ray production from switching impulses in detail.

However, as concluding remarks, we can state that switching impulses, where the voltage rise-time is very much slower compared to lightning impulses, do produce X-rays and the mechanism proposed in by Cooray et al. in [22] could still be valid for switching impulses. It is also important to mention that any direct correlation of X-ray production with the rate of change of supplied voltage as observed in [20] is not compatible with the results of this experiment.

5. Conclusions

Conclusions based on our findings are as follows.

1) Paper I

The experimental work conducted in this study shows that the energy of X-ray bursts generated by 1 m long laboratory sparks of negative polarity increases with decreasing anode radius. This observation is in support of the theory proposed by Cooray et al. in [22] but may not explain all experimental observations yet.

2) Paper II

The experimental data presented in this paper, in combination with a simple attenuation based numerical model, show that the maximum energy of the X-ray photons generated in 1 m long negative sparks is in the order of 200 keV to 250 keV with mean energy around 50 keV to 55 keV. The two types of distributions considered produce similar results for the mean energy and the total number of photons. Despite being slightly different from previous estimates reported in [21], [23], [27], [28], the values derived in this study, are of the same order of magnitude as these previous estimates.

3) Paper III

In this paper, the extremely low occurrence of X-rays at ground level due to subsequent return strokes of upward initiated lightning from Gaisberg Tower in Austria located at a high altitude is presented. This is in contrast to the observations made in triggered lightning. Previous studies show that the X-ray emissions are controlled by the electric field at the tip of the dart leaders. This electric field is related to the charge accumulated at the tip of the dart leader. Since the charge accumulated at the tip of the dart leader increases with increasing length of the dart leader channel, it is suggested that the weak X-ray emissions are probably due to the shorter dart leader channels associated with the lightning flashes striking the Gaisberg Tower or due to the modification of the lightning channel by long continuing leaders.

4) Paper IV

X-rays from switching impulse laboratory discharges are reported for the first time. X-rays seem to appear before the complete breakdown during the final jump (attachment process). Since the X-ray energies obtained in switching impulses are comparable to those observed when using lightning impulses, the results show that the slow rise-time of switching voltage impulse does not have a significant influence on the production of X-rays. The results also indicate that X-ray emissions are taking place just before the breakdown, strengthening the possibility that the mechanism of X-ray production is related to the encounter between streamers of opposite polarity.

6. Future Work

Future work and recommendations concerning X-ray detection from laboratory discharges and upward initiated lightning.

Very long laboratory sparks: Almost all the experiments pertinent to X-ray generation from laboratory sparks, including the ones presented in this thesis, have been conducted with sparks gaps in the order of 1 m or shorter. Compared to lightning and very long laboratory sparks of few meters, the breakdown process taking place in shorter gaps could be considered as primarily mediated by streamers. However, for longer gaps, both leaders and streamers are present prior to breakdown and these sparks are more analogues to lightning. Because of this significant difference of breakdown mechanism, the study of X-ray measurements from very long gaps is highly recommended. Even in the case of switching impulses, which are more likely to produce leaders for a given gap length, the shorter gaps are more likely to produce streamer only breakdowns. The other advantage of very long laboratory discharges is the following. Due to their longer time to breakdown, and also because of the possible involvement of leaders, each step in a breakdown mechanism is separated more in both time and space. Consequently, a better correlation of X-ray emissions with the various events in the process of breakdown would be possible.

More switching impulse tests: The X-ray emission from laboratory sparks with switching impulses were reported in Paper IV for the first time. However, in this test, because of time constraints, only a few sparks were applied. Thus, similar to the tests conducted for lightning impulses, more elaborate tests with switching impulses should be conducted.

More measurement parameters – HV current & high-speed videography:

In X-ray related laboratory experiments, the correlation of X-ray emission to the current from each electrode is a critical parameter. This is due to the fact that the current is related to the charge in streamers and leaders which, in turn, is related to the background electric field. In the experiments conducted in this thesis work current was measured only at the ground electrode. Therefore, a more sensitive current measurement also on the high voltage side is highly recommended. Similarly, the high-speed videography could also be used to obtain photographic evidence for the physical mechanism behind the X-ray generation.

X-ray detection from upward initiated lightning: The dart or dart-stepped leaders in upward initiated lightning are reported to generate far fewer X-rays compared to natural or triggered-lightning from the study conducted in Paper III. However in order to confirm this finding more experiments in other tall structures in both high and low altitude should be conducted. In order to maximize the detection possibility, more X-ray detectors can be utilized. The use of more detectors, would also help to counteract any anisotropic emission of X-rays.

Svensk Sammanfattning

År 1925 förutspådde nobelpristagaren R. C. Wilson att stora elektriska fält av åskväder skulle kunna accelerera elektroner till relativistiska energier som kan generera röntgenstrålar och gammastrålar genom bromsstrålning från åskväder. Den första upptäckten av röntgen från blixten gjordes 2001 och den första upptäckten av gammastrålar från åskväder gjordes år 1994. Den första upptäckten av röntgenstrålar i långa gnistor gjordes 2005. Sedan dess lyckades ett stort antal experimentella undersökningar kvantifiera den rumsliga och tidsmässiga fördelningen av röntgenstrålar och gammastrålar som genereras av åskväder, blixtnedslag och långa laboratoriegnistor. Dessa studier ledde till en betydande förbättring av vår förståelse för hur elektroner accelereras till relativistiska energier både i åskväder, blixtnedslag och långa laboratoriegnistor. Trots dessa upptäckter finns det fortfarande luckor i vår kunskap om produktion av röntgenstrålar från blixtnedslag och långa gnistor och motivationen i denna avhandling var att rätta till denna situation genom att utföra nya experiment för att samla in data inom de ämnesområden där information fortfarande saknas.

Den tidsmässiga och rumsliga variationen i utvecklingen av urladdningen i långa laboratoriegnistor beror på elektrodgeometrin. Det första problemet som vi har att ta upp i denna avhandling är att förstå hur elektrodgeometrin påverkar genereringen av röntgenstrålar. De erhållna resultaten visar att elektrodgeometrin påverkar röntgengenerationen och vi lyckades visa att detta beroende kunde förklaras med en modell som tidigare utvecklats av forskare vid Uppsala universitet. Den andra informationen om röntgengenerering från långa gnistor som saknades under början av detta avhandlingsarbete är kunskapen om fördelningen av energi av röntgenfoton i röntgenskurar. Med hjälp av en serie dämpare lyckas vi observera hur röntgenfotonerna dämpas som en funktion av barriärtjocklek och genom att använda en ganska enkel modell som bara innehåller några variabler lyckas vi få medel och den maximala energin som är associerad med röntgenfoton.

Laboratorieurladdningar skulle kunna framställas av både kort- och långimpulser, men alla studier som genomfördes före detta avhandlingsarbete var baserade på de korta blixtpulserna. Utvecklingen av den elektriska urladdningen är annorlunda när laboratoriegnistor framställs antingen genom de korta blixtpulserna eller de långa så kallad omkopplingsimpulserna. Vid omkopplingsimpulser stiger spänningssvågen väldigt långsamt i jämförelse med blixtpulsen och vissa forskare har lagt fram teorier för att föreslå att

stigningstakten är en viktig parameter i röntgenutveckling. Vår studie visar för första gången att även om stigningstakten för omkopplingsimpulser är hundratal gånger långsammare än bliximpulser, är omkopplingsimpulser lika effektiva som bliximpulser för att generera röntgenstrålar. Vi visade igen att detta stämmer överens med den teori som tidigare utvecklats av Uppsala forskare.

Blixtnedslag som slår mot marken kan delas upp i nedåtgående och uppåtgående blixtar. Uppåtriktade blixtar initieras av långa strukturer som påverkas av elektriska fält under åskväder. Förutom dessa naturliga kategorier lyckas även forskare skapa blixtnedslag genom att skicka raket med släpade metalltrådar mot moln. Dessa kallas utlösande blixtnedslag. Alla observationer om röntgengenerering från blixten vid tidpunkten för början av denna avhandling baserades på antingen naturliga nedåtgående blixurladdningar eller utlösande blixtnedslag i Florida. De första experimenten att studera röntgengenerering från uppåtriktade blixurladdningar utfördes systematiskt inom detta avhandlingsarbete vid Gaisberg-tornet i Österrike. Resultaten visade att röntgenutstrålningen från dessa blixtar är mycket svagare än de som produceras av antingen naturligt nedåtriktat eller utlösande blixtnedslag. Ett försök görs för att förklara denna observation genom att åberopa de möjliga skillnaderna i laddningsfördelningen för ledare som är förknippade med de utlösande blixterna i Florida och uppåtriktade blixtnedslagen vid Gaisberg-tornet.

Acknowledgements

First and foremost, I would like to express my deepest gratitude to my supervisor Professor Vernon Cooray for the immense support and guidance provided throughout the study, for his patience, motivation, and the belief he had on me and my strengths. It has been a great honour and pleasure being a student of a great scientist like him. I could not have imagine having a better mentor.

Secondly, I wish to convey my sincere thanks to my co-supervisor, friend, and mentor, Associate Professor Dr. Mahbubur Rahman for his insightful guidance, sharing his expertise on HV engineering, encouragement and support in overcoming numerous obstacles during my research. I am also grateful to him for providing the ‘Svensk Sammanfattningen’.

I am also thankful to my co-supervisor Professor Mats Leijon for his advices and guidance and also the Division of Electricity for funding my research and giving the opportunity to conduct a PhD in Uppsala University.

I would also like to specially thank Dr. Liliana Arevalo, for the guidance and support she has given me, and also for funding my research through ABB AB.

I would also like to specially thank Professor I.M.K.Fernando of University of Colombo, Sri Lanka, who provided me the opportunity to join this research group and has being a constant supporter of my research work throughout the years.

I would like to thank my friends Zikri, Liliana, Azlinda, Mona, Saman, Juan de S., Riduan, Marcus B., Oscar, Dalina, Muzafar, Andre, Nasir, Victor M., and many other past and present members of our division of electricity for their feedback, cooperation and of course their friendship. I have had a great time in Uppsala, in your company.

I am thankful for to the present and former personnel at the Division of Electricity and the Department of Engineering Science: Thomas Götschl, Ingrid Ringård, Maria Skoglund, Gunnel Ivarsson, Ulf Ring, Emma Holmberg, Anna Wiström, Maria Nordengren, Lena Gamova, and many others for their administrative and technical support to conduct my studies and research.

I would like to convey my gratitude to my friends in Upppsala; Wimal, Kumari, Sanjeewani, Kasun, Lalith, Samanthi, Shiran and others who made our stay in Uppsala remarkable with all the dinners, movies and late-night discussions and especially for their willingness to help whenever I needed.

I am indebted to my loving mother and late father, who have provided me through moral and emotional support in my life and who are immensely proud of my achievements.

I am ever grateful and happy for you, my two princesses Mehasna and Kinuli for your smiles, laughs, and for being my inspiration every day, and to simply have you in my life.

Last but not least, I would like to thank my dear wife, my friend, and my partner, Muditha, who has continuously been with me for the past years and giving me constant support and love in my life. Without her support, this PhD would have been impossible to complete. And I must also thank her for creating those beautiful vector graphics used in my research articles.

References

- [1] J. R. Dwyer, D. M. Smith, and S. A. Cummer, “High-energy atmospheric physics: Terrestrial gamma-ray flashes and related phenomena,” *Space Sci. Rev.*, vol. 173, no. 1–4, pp. 133–196, 2012.
- [2] G. J. Fishman *et al.*, “Discovery of Intense Gamma-Ray Flashes of Atmospheric Origin,” *Science*, vol. 264, no. 5163, pp. 1313–1316, 1994.
- [3] M. S. Briggs *et al.*, “First results on terrestrial gamma ray flashes from the Fermi Gamma-ray Burst Monitor,” *J. Geophys. Res. Sp. Phys.*, vol. 115, no. A7, 2010.
- [4] M. Tavani *et al.*, “Terrestrial Gamma-Ray Flashes as Powerful Particle Accelerators,” *Phys. Rev. Lett.*, vol. 106, no. 1, p. 18501, Jan. 2011.
- [5] O. Chanrion and T. Neubert, “Production of runaway electrons by negative streamer discharges,” *J. Geophys. Res. Sp. Phys.*, vol. 115, no. A6, 2010.
- [6] M. S. Briggs *et al.*, “Electron-positron beams from terrestrial lightning observed with Fermi GBM,” *Geophys. Res. Lett.*, vol. 38, no. 2, 2011.
- [7] J. R. Dwyer *et al.*, “A ground level gamma-ray burst observed in association with rocket-triggered lightning,” *Geophys. Res. Lett.*, vol. 31, no. 5, 2004.
- [8] J. R. Dwyer *et al.*, “Observation of a gamma-ray flash at ground level in association with a cloud-to-ground lightning return stroke,” *J. Geophys. Res. Sp. Phys.*, vol. 117, no. 10, 2012.
- [9] K. B. Eack, D. M. Suszcynsky, W. H. Beasley, R. Roussel-Dupre, and E. Symbalisty, “Gamma-ray emissions observed in a thunderstorm anvil,” *Geophys. Res. Lett.*, vol. 27, no. 2, pp. 185–188, Jan. 2000.
- [10] V. V. V Alexeenko, N. S. S. Khaerdinov, A. S. S. Lidvansky, and V. B. B. Petkov, “Transient variations of secondary cosmic rays due to atmospheric electric field and evidence for pre-lightning particle acceleration,” *Phys. Lett. A*, vol. 301, no. 3–4, pp. 299–306, Aug. 2002.
- [11] G. D. Moss, V. P. Pasko, N. Liu, and G. Veronis, “Monte Carlo model for analysis of thermal runaway electrons in streamer tips in transient luminous events and streamer zones of lightning leaders,” *J. Geophys. Res.*, vol. 111, no. A2, 2006.

- [12] J. R. Dwyer, "The relativistic feedback discharge model of terrestrial gamma ray flashes," *J. Geophys. Res. Sp. Phys.*, vol. 117, no. A2, Feb. 2012.
- [13] A. V Gurevich, G. M. Milikh, and R. Roussel-Dupre, "Runaway electron mechanism of air breakdown and preconditioning during a thunderstorm," *Phys. Lett. A*, vol. 165, no. 5–6, pp. 463–468, 1992.
- [14] C. T. R. Wilson, "The Acceleration of β -particles in Strong Electric Fields such as those of Thunderclouds," *Math. Proc. Cambridge Philos. Soc.*, vol. 22, no. 4, p. 534, 1925.
- [15] C. B. Moore, K. B. Eack, G. D. Aulich, and W. Rison, "Energetic radiation associated with lightning stepped-leaders," *Geophys. Res. Lett.*, vol. 28, no. 11, pp. 2141–2144, 2001.
- [16] J. R. Dwyer, "Energetic Radiation Produced During Rocket-Triggered Lightning," *Science (80-.)*, vol. 299, no. 5607, pp. 694–697, 2003.
- [17] J. R. Dwyer, H. K. Rassoul, Z. Saleh, M. A. Uman, J. Jerauld, and J. A. Plumer, "X-ray bursts produced by laboratory sparks in air," *Geophys. Res. Lett.*, vol. 32, no. 20, 2005.
- [18] M. Rahman, V. Cooray, N. A. Ahmad, J. Nyberg, V. A. Rakov, and S. Sharma, "X rays from 80-cm long sparks in air," *Geophys. Res. Lett.*, vol. 35, no. 6, 2008.
- [19] C. V. Nguyen, A. P. J. van Deursen, and U. Ebert, "Multiple x-ray bursts from long discharges in air," *J. Phys. D. Appl. Phys.*, vol. 41, no. 23, p. 234012, 2008.
- [20] V. March and J. Montanyà, "Influence of the voltage-time derivative in X-ray emission from laboratory sparks," *Geophys. Res. Lett.*, vol. 37, no. 19, 2010.
- [21] P. O. Kochkin, C. V Nguyen, A. P. J. van Deursen, and U. Ebert, "Experimental study of hard x-rays emitted from metre-scale positive discharges in air," *J. Phys. D. Appl. Phys.*, vol. 45, no. 42, p. 425202, Oct. 2012.
- [22] V. Cooray, L. Arevalo, M. Rahman, J. Dwyer, and H. Rassoul, "On the possible origin of X-rays in long laboratory sparks," *J. Atmos. Solar-Terrestrial Phys.*, vol. 71, no. 17–18, pp. 1890–1898, 2009.
- [23] P. O. Kochkin, A. P. J. Van Deursen, and U. Ebert, "Experimental study on hard x-rays emitted from metre-scale negative discharges in air," *J. Phys. D. Appl. Phys.*, vol. 48, no. 2, Jan. 2014.
- [24] P. Kochkin, N. Lehtinen, A. P. J. Van Deursen, and N. Østgaard, "Pilot system development in metre-scale laboratory discharge," *J. Phys. D. Appl. Phys.*, vol. 49, no. 42, p. 425203, 2016.
- [25] J. R. Dwyer *et al.*, "A study of X-ray emission from laboratory sparks in air at atmospheric pressure," *J. Geophys. Res.*, vol. 113, no. D23, p. D23207, 2008.
- [26] V. March and J. Montanyà, "X-rays from laboratory sparks in air: The role of the cathode in the production of runaway electrons," *Geophys. Res. Lett.*, vol. 38, no. 4, 2011.

- [27] B. E. Carlson *et al.*, “Meter-scale spark X-ray spectrum statistics,” *J. Geophys. Res. Atmos.*, vol. 120, no. 21, pp. 11191–11202, 2015.
- [28] P. Kochkin, C. Köhn, U. Ebert, and L. van Deursen, “Analyzing x-ray emissions from meter-scale negative discharges in ambient air,” *Plasma Sources Sci. Technol.*, vol. 25, no. 4, p. 44002, 2016.
- [29] J. R. Dwyer *et al.*, “X-ray bursts associated with leader steps in cloud-to-ground lightning,” *Geophys. Res. Lett.*, vol. 32, no. 1, 2005.
- [30] Z. Saleh *et al.*, “Properties of the X-ray emission from rocket-triggered lightning as measured by the Thunderstorm Energetic Radiation Array (TERA),” *J. Geophys. Res.*, vol. 114, no. D17, 2009.
- [31] S. Mallick, V. A. Rakov, and J. R. Dwyer, “A study of X-ray emissions from thunderstorms with emphasis on subsequent strokes in natural lightning,” *J. Geophys. Res. Atmos.*, vol. 117, no. D16, 2012.
- [32] J. Montanyà *et al.*, “Registration of X-rays at 2500 m altitude in association with lightning flashes and thunderstorms,” *J. Geophys. Res. Atmos.*, vol. 119, no. 3, pp. 1492–1503, Feb. 2014.
- [33] P. O. Kochkin, A. P. J. J. Van Deursen, and U. Ebert, “Experimental study of the spatio-temporal development of metre-scale negative discharge in air,” *J. Phys. D. Appl. Phys.*, vol. 47, no. 14, p. 145203, 2014.
- [34] J. H. Hubbell and S. M. Seltzer, “X-Ray Mass Attenuation Coefficients - NISTIR 5632,” 2004. [Online]. Available: <https://physics.nist.gov/PhysRefData/XrayMassCoef/tab3.html>. [Accessed: 05-Jan-2018].
- [35] G. Diendorfer, H. Pichler, and M. Mair, “Some Parameters of Negative Upward-Initiated Lightning to the Gaisberg Tower (2000–2007),” *IEEE Trans. Electromagn. Compat.*, vol. 51, no. 3, pp. 443–452, Aug. 2009.
- [36] H. Zhou, G. Diendorfer, R. Thottappillil, H. Pichler, and M. Mair, “Characteristics of upward bipolar lightning flashes observed at the Gaisberg Tower,” *J. Geophys. Res.*, vol. 116, no. D13, p. D13106, Jul. 2011.

Acta Universitatis Upsaliensis

*Digital Comprehensive Summaries of Uppsala Dissertations
from the Faculty of Science and Technology 1618*

Editor: The Dean of the Faculty of Science and Technology

A doctoral dissertation from the Faculty of Science and Technology, Uppsala University, is usually a summary of a number of papers. A few copies of the complete dissertation are kept at major Swedish research libraries, while the summary alone is distributed internationally through the series Digital Comprehensive Summaries of Uppsala Dissertations from the Faculty of Science and Technology. (Prior to January, 2005, the series was published under the title "Comprehensive Summaries of Uppsala Dissertations from the Faculty of Science and Technology".)

Distribution: publications.uu.se
urn:nbn:se:uu:diva-338158



ACTA
UNIVERSITATIS
UPSALIENSIS
UPPSALA
2018